Master's thesis

NTNU
Norwegian University of Science and Technology
Faculty of Economics and Management
Department of Industrial Economics and Technology Management

Jørgen Gustavsen
Ole-Andreas Sandnes

Convertible Bond Arbitrage with the AFV Model

An empirical assessment of delta hedging capability

Master's thesis in Industrial Economics and Technology Management
Supervisor: Einar Belsom
June 2019

NTNU
Norwegian University of Science and Technology

Jørgen Gustavsen
Ole-Andreas Sandnes

Convertible Bond Arbitrage with the AFV Model

An empirical assessment of delta hedging capability

Master's thesis in Industrial Economics and Technology Management
Supervisor: Einar Belsom
June 2019

Norwegian University of Science and Technology
Faculty of Economics and Management
Department of Industrial Economics and Technology Management

NTNU
Norwegian University of
Science and Technology

Abstract

We perform an empirical analysis of the convertible bond model proposed by Ayache-Forsyth-Vetzal, calibrated with the method proposed by Andersen & Buffum, with the intent of testing the model's applicability to convertible arbitrage strategies. We backtest the model for two publicly traded convertible bonds between 2018-02-01 and 2019-04-23 and analyze the effectiveness of the model delta by comparing quantile correlations of the convertible bond with the underlying stock to those of a delta-hedged portfolio with the underlying stock. An effective delta hedge should result in a substantial reduction in the correlation for quantiles covering small stock returns, and ideally this correlation should be zero. We find that whereas the model is able to fit closely to market prices, the deltas from the model do not match those of the market. We observe that for the two bonds in our sample, the deltas from the model are about twice as large as the deltas that would give the best delta hedge in the selected trading period, and by multiplying the model deltas by a constant tuning factor we are able to obtain mid 80% quantile correlations much closer to zero.

Sammendrag

Vi utfører en empirisk analyse av prisingsmodellen for konvertible obligasjoner foreslått av Ayache-Forsyth-Vetzal, kalibrert med metoden beskrevet av Andersen & Buffum, med mål om å teste modellens anvendelighet i *convertible arbitrage*-strategier. Vi tester modellen for to børsnoterte konvertible obligasjoner i perioden 01.02.2018-23.04.2019 og analyserer hvor effektiv modellen er ved å sammenligne kvantilkorrelasjoner mellom obligasjonen og den underliggende aksjen med kvantilkorrelasjoner mellom en hedget portefølje og den underliggende aksjen. En effektiv delta-hedge bør resultere i en betydelig reduksjon i korrelasjon for kvantiler som dekker små kursendringer i aksjen, og ideelt sett bør denne korrelasjonen være null. Vi finner at modellen produserer priser som avviker lite fra markedspriser, men at modellens deltaer avviker betydelig fra deltaer observert i markedet. For de to obligasjonene i vårt utvalg finner vi at modellens deltaer er omtrent dobbelt så store som de deltaer som ville gitt den beste delta-hedgen i den utvalgte tidsperioden, og ved å multiplisere modelldeltaene med en konstant endringsfaktor oppnår vi kvantilkorrelasjoner for den midterste 80%-kvantilen svært nær null.

Preface

This thesis concludes our Master of Science in Industrial Economics and Technology Management with specialization in Financial Engineering at NTNU. Studying quantitative finance has been both inspiring and challenging. The field lies at the intersection of finance, computer science, mathematics and statistics, all of which are academic disciplines we find interesting. From an initial interest in bonds and options pricing this thesis has taken us deep into the complex mathematics behind convertible bonds and the challenges associated with numerical solution methods, a journey that has been both frustrating and rewarding. We hope the reader will find this thesis interesting, and perhaps get inspired to explore the topic of convertible arbitrage further.

We would like to express our sincere gratitude towards our supervisor, Einar Belsom, associate professor at the Department of Industrial Economics and Technology Management at NTNU, for his valuable input during the writing process. We would also like to thank Espen Robstad Jakobsen, professor at the Department of Mathematical Sciences at NTNU, for suggesting upwind discretization as a solution to our problems with the calibration of the model.

Contents

List of Figures

List of Tables

Chapter 1

Introduction

When firms need to raise capital they can choose among equity, debt or hybrid securities, which combine equity and debt components. In this thesis we focus on convertible bonds, a type of hybrid instrument which displays both equity- and bond-like features.

Convertible bonds (CB) have been around for the past 150 years, and started as a source of capital for U.S. railroad companies. Today, however, 32.5% of all convertibles are issued by the tech sector (Gabelli, 2018), followed by consumer discretionary, financial companies and the health care sector. The full sector exposure of the CB market as well as the CB market size is shown in Table 1.1. The investors in CBs can be divided into two types: long-only and hedged. As of 2Q18 65% of US CBs and 70% of European CBs are owned by long-only investors, meaning that the rest is owned by hedge funds. There have, however, been periods in which hedge funds dominated the CB market (Gabelli, 2018).

A common strategy used by hedge funds is *convertible bond arbitrage*. The strategy consists of a long position in the convertible bond and a short position of *delta* shares in the underlying stock, resulting in a delta neutral position. The delta is the first derivative of the CB price with respect to stock price, i.e. the change in CB price per change in the underlying stock, and gamma is the second-derivative with respect to stock price, i.e. the change in delta per change in the underlying stock. For small changes in the stock price, the net payoff of the position will be unchanged. However, if the gamma is positive, the

Table 1.1: Convertible Market Sector Exposure. Source: Barclay's June 30, 2018

Equity Sector	Market Cap. (USDb)	Percentage of Market
Consumer Discretionary	41.7	18.7 %
Consumer Staples	3.5	1.5%
Energy	14.0	6.3%
Financials	33.4	15.0%
Health Care	33.2	14.8%
Industrials	10.2	4.6%
Information Technology	72.6	32.5%
Materials	3.9	1.8%
Telecommunication Services	2.0	0.9%
Utilities	9.0	4.0%
Total	223.5	100%

position will yield a positive return for large price jumps in the underlying stock no matter the direction. A positive gamma means that as the stock price increases, the CB increases more in value than the short position loses. If the stock price falls, then the CB falls less in value than is gained from the short position. Convertible arbitrageurs generally look for equity-like convertible bonds. The underlying shares have a higher volatility, which translates into a higher value for the equity option, a lower conversion premium, and a higher gamma. Moreover, convertible arbitrageurs prefer underlying stocks that (1) pay low or no dividends, (2) are undervalued, (3) are liquid, and (4) can easily be sold short (Loncarski et al., 2009). In the 1990's CB arbitrage-indices had annual returns between 10-20% (Loncarski et al., 2009).

Another interesting feature of CBs is that they tend to perform well during periods of rising interest rates (Gabelli, 2018). This feature can be observed in Figure 1.1, where the performance of different asset classes in periods with rising interest rates is presented. A reason for these performances may be that the sectors that dominate the CB market are typical growth markets, which are likely to perform well during periods of economic expansion, which often experience rising interest rates. Another reason may be that the duration of CBs are typically lower than on non-convertible bonds, which lowers the exposure to credit risk.

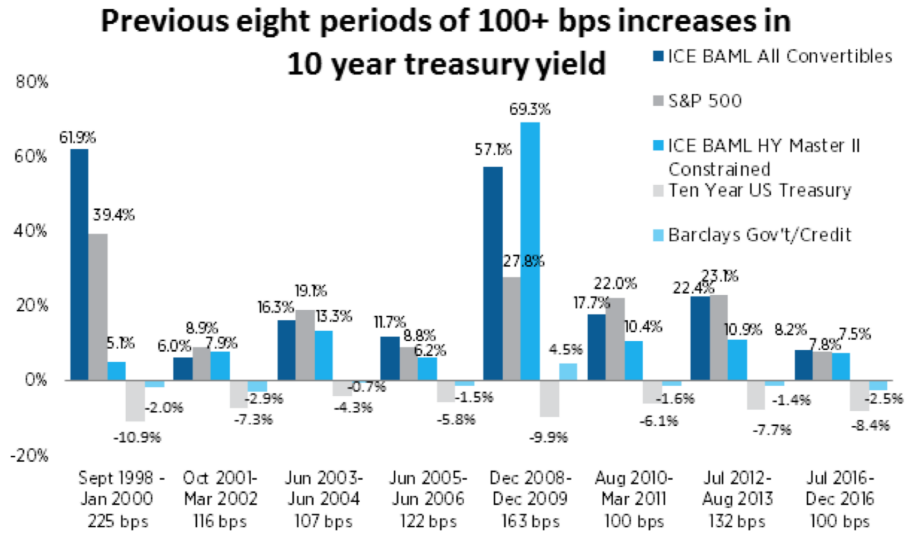

Figure 1.1: Historical performance of different asset classes in a rising rate environment. Source: (Gabelli, 2018, p. 7)

The typical shape of the price curve of a convertible is depicted in Figure 1.2. For low stock prices the debt is distressed and trades at a steep discount to investment value. When the debt is no longer distressed the CB moves into the *out-of-the-money* area, where the CB is more sensitive to the bond component due to low option value. For increasing stock prices the convertible bond moves into the *at-the-money* area where the embedded option influence the CB more and more, and in the *in-the-money* area the price of the convertible converges to *parity* where it will be exercised immediately. Parity is simply the stock price multiplied by the conversion ratio, and constitutes the value of the convertible bond after conversion.

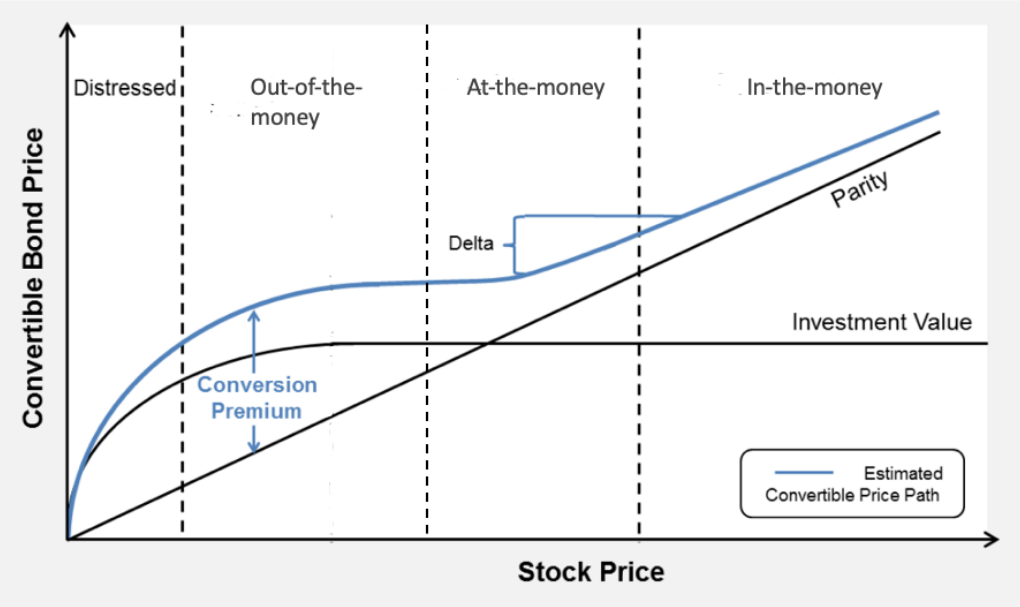

Figure 1.2: Convertible bond price curve

The literature on convertibles begins with valuation of CBs based on valuation of non-convertible debt (e.g. Merton (1974), combined with Black and Cox (1976)) and Black and Scholes (1973) framework for valuing options. Ingersoll Jr (1977) and Brennan and Schwartz (1980) were among the first to derive valuation models for CBs. Later, models were derived to take different features into account. Such features are for example that the issuing company can call back the bond at a certain price at a particular time in the future, or that the investor can choose to put the bond (sell it back to the issuer) at a predetermined price. Brennan and Schwartz (1977) derived a valuation model and optimal strategies for call and conversion, while GoldmanSachs (1994) takes both call and put features into account in their model.

One aspect of the different components of convertible bonds is that they are subject to different credit risks. Tsiveriotis and Fernandes (1998) argued that the equity part of the CB is not subject to credit risk, because the company can always provide its own stock, whereas the bond part in nature is subject to credit risk. Splitting the CB into two parts, leads to a pair of coupled partial differential equations, which can be solved using finite differences. The research note by GoldmanSachs (1994) takes the same problem into account by estimating the probability of conversion at some point, and then setting the discount rate to the weighted average of risk free rate and the risk free rate plus credit spread, where the probability of conversion is the weighting factor. Ammann et al. (2008) proposed a method for pricing convertible bonds using Monte Carlo simulation. This allows for better modeling of a rich set of real-world specifications that are hard to specify in a binomial tree or a closed form model.

In recent literature Ayache et al. (2003) expanded Tsiveriotis-Fernandes' model ("TF model") to take default risk into account and see what happens to the price of the CB in the event of default by the issuing firm. Ayache et al. (2003) claims that Tsiveriotis-Fernandes' model is internally inconsistent, and that "Tsiveriotis and Fernandes (1998) provide no discussion of the actual events in the case of default, and how this would affect the hedging portfolio. There is no clear statement in their paper as to what happens to the stock price in the event of default"(Ayache et al., 2003, p. 10). Because the TF-model does not specify what happens in case of default, one cannot generate a self-financing and risk-free hedging portfolio. By taking the probability of default and what happens in case

of default into account, Ayache et al. (2003) develop a new pricing model ("AFV model") that can be used to generate a zero risk and self-financing hedging portfolio. To use this model on a real case one has to use market data on options and default probability, such as zero coupon bonds or CDS-contracts, to calibrate the input parameters. The calibration process is described by Andersen and Buffum (2002), who suggest that applying the calibration theory in practice is a "challenging and interesting avenue for future research".

There is some literature empirically testing pricing, but with many different pricing models there is not extensive literature testing each model. We also find the literature lacking in assessing the hedging capability of different models. Zabolotnyuk et al. (2010) empirically test the pricing capability of the Ayache-Forsyth-Vetzal model, the same model as in this thesis, but do not test hedging. They find a very small model overpricing of 0.35% on 64 convertible bonds on the Toronto Exchange. However, they do not calibrate the model using the Andersen and Buffum (2002) methodology, but instead use the Marquardt algorithm to select model parameters that closely fit model prices to historical convertible bond prices. This methodology could lead to overfitting, which would yield low pricing errors. We notice that their estimated mean recovery rate is a mere 1%, which we find unrealistic. They also let the p-parameter in Equation 2.6, which governs the stock price dependent behavior of the credit spread, vary from 5.91 to -4.81. Letting p be negative implies that an increase in stock price yields an increase in credit spread, which is also unrealistic. Such a low recovery rate will, in combination with an unconstrained p, give the algorithm more freedom to tune other parameters to get the desired price range, but will affect the delta and gamma.

Ammann and Seiz (2006) do an empirical assessment of both pricing and hedging mandatory convertible bonds, but they assess a different model than the AFV model. Mandatory convertibles are mandatorily converted into common stock at maturity, unlike regular convertible bonds. Ammann and Seiz (2006) find low pricing and hedging errors, however, due to the inherent differences between mandatory convertibles and regular convertibles the papers results are not comparable to our study.

This thesis adds to the literature on convertible bonds by assessing the hedging performance of the Ayache-Forsyth-Vetzal model (Ayache et al., 2003), calibrated with the method presented by Andersen and Buffum (2002). This is the model outlined in the

Bloomberg OVCV model description (David Frank, 2018), a widely used financial software program.

Ideally we would like to do an empirical study of all the greeks in the AFV model. However, the greeks will be practically unobservable as the convertible bond is less liquid than the underlying stock, and there could be a change in several of the relevant input parameters such as volatility and credit spread for every observed price change of the convertible bond. Hence it is logical to focus the empirical assessment on delta, the greek that is most commonly hedged.

To do this we backtest a delta hedged portfolio of two convertible bonds to analyze the performance. To assess the effectiveness of the delta hedge we compare the level of correlation of the convertible bond with the underlying stock to the correlation between a delta hedged portfolio and the underlying stock. By quantifying the decrease in correlation we can evaluate the effectiveness of the hedge. We further do an analysis of the correlations in different quantiles of stock returns to better capture the delta hedging effect, which only works for small changes in the underlying stock. We also fit a second degree polynomial to the absolute value of the hedging error on stock returns to check whether the gamma effect, which is not hedged in delta-hedging, has some explanatory power in the hedging error. Hence, we test whether the AFV model is suitable to hedging the risk associated with small price changes in the underlying stock, and test whether residual stock price risk is due to the convexity of the convertible bond. Confirmation of this would imply that the AFV model is suitable as a model for delta hedging and engaging in convertible arbitrage strategies.

The remaining chapters are organized as follows: Chapter 2 presents the model and calibration method, Chapter 3 presents the data sources and sample selection and Chapter 4 presents each bond case and contains the pricing and hedging results. Chapter 5 discusses the results obtained in Chapter 4 and presents possible explanations of the deviations from the market. Lastly, Chapter 6 concludes the analysis of the delta hedging performance and suggests possible avenues for further research.

Chapter 2

Model

The model analyzed in this thesis is the Hedging Model proposed by Ayache et al. (2003) ("AFV model"). This model extends and improves the model proposed by Tsiveriotis and Fernandes (1998)("TF model") by including default risk and describing what happens in the case of default. The AFV model does not split the CB in the same way as TF, thus it manages to avoid some of the numerical problems around the point of conversion. Ayache et al. (2003) show that the TF framework can result in a situation where a call by the issuer just before expiry renders the CB independent of credit risk, and situations where the risk-neutral hedged portfolio is not self-financing, and hence is not suitable for pricing or hedging convertible bonds.

We implement the AFV model with the calibration procedure proposed by Andersen and Buffum (2002) because this is the model used by Bloomberg (David Frank, 2018), a widely used financial software. Due to Bloomberg's popularity we assume that quoted market prices for convertible bonds should be close to those produced by Bloomberg's OVCV tool.

2.1 The AFV Model

The Hedging Model proposed by Ayache et al. (2003) assumes that stock prices follow a risk-neutral jump-diffusion process:

$$dS = (r + \lambda\eta - \delta)Sdt + \sigma Sdz - \eta Sdq \tag{2.1}$$

where r is the risk-free rate, δ is the dividend rate and η denotes the loss rate for equity owners in case of default which we assume to be absolute, i.e. $\eta = 1$. dz is a Wiener process and dq is a Poisson process given by:

$$dq = \begin{cases} 1, & \text{probability } \lambda dt \\ 0 & \text{probability } (1 - \lambda dt) \end{cases} \tag{2.2}$$

The term $\lambda\eta$ is a term added to the drift in Equation 2.1 to compensate for the expected downward drift from the jump term, $E_r[-dq] = -\lambda\eta dt$, and makes the stock price dynamic risk-neutral. The drift compensation makes the process satisfy the arbitrage restriction that $S(t)e^{-\int_0^t [r(u)-\delta(u)]du}$ be a *martingale* under the risk-neutral probability measure (Andersen and Buffum, 2002), i.e. a stochastic process for which the conditional expectation of the next value is equal to the present value.

The inclusion of the Poisson process enables the modeling of default risk and incorporation of time-varying volatility effects, which is not possible in earlier models such as Tsiveriotis and Fernandes (1998) and GoldmanSachs (1994). Under this price dynamic, the system of SPDEs to be solved is the following:

$$C_t = -\left(\frac{\sigma^2}{2}S^2 C_{SS} + (r + \lambda\eta - \delta)SC_S - (r + \lambda)C\right) - \lambda \max[\kappa S(1 - \eta) - RF, 0] \tag{2.3}$$

$$B_t = -\left(\frac{\sigma^2}{2}S^2 B_{SS} + (r + \lambda\eta - \delta\right)SB_S - (r + \lambda)B) - \lambda RF \tag{2.4}$$

$$V_t = C_t + B_t \tag{2.5}$$

where V_t is the model price of the CB, C_t is the option component at time t, B_t is the bond component at time t, κ denotes the conversion ratio, R is the recovery rate and F is

the face value. These equations are then discretized and solved for using finite difference methods, more specifically the Crank-Nicolson numerical scheme. The derivation and discretization of these equations, the boundary conditions, and the final Crank-Nicolson scheme are found in the Appendix. Solving the scheme over all timesteps and stock prices yields the price surface shown in Figure 2.1.

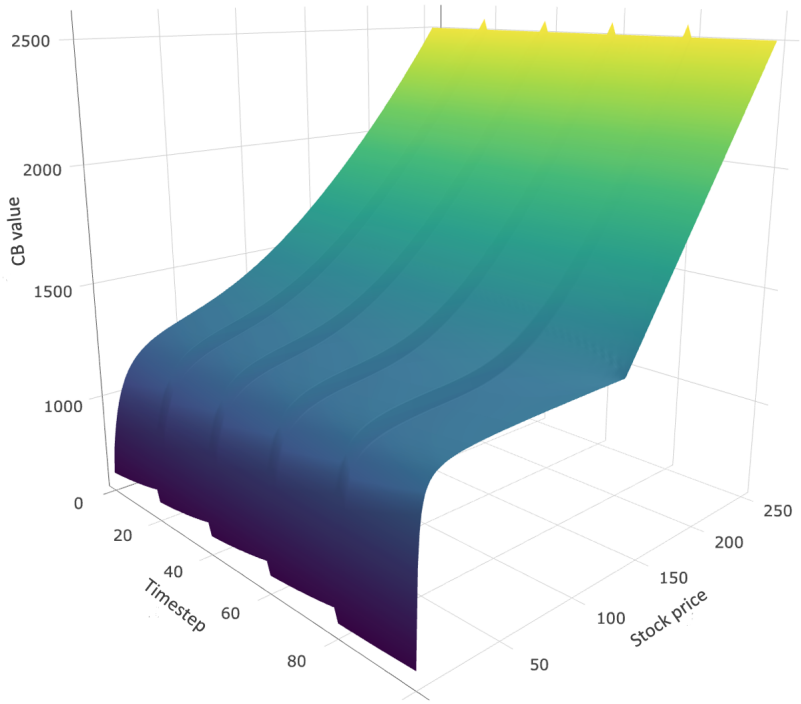

Figure 2.1: Convertible bond price surface. Maturity is at last timestep. As seen the price drops to the assumed recovery rate when stock prices go to zero

2.2 Calibration

Both implied option volatility and credit spreads depend in a complicated way on maturity and the joint parameterization of $\lambda(t, S)$ and $\sigma(t, S)$. A straight-forward parameterization with constant volatility and time-invariant intensity $\lambda(S) = c(\frac{S(0)}{S})^p$ can create highly non-flat, non-monotonic and unrealistic term structures of implied volatility and credit spreads. Using time-dependent functions for both $\lambda(t, S)$ and $\sigma(t, S)$ as given in Equation 2.6 and Equation 2.7 allows the modeling of a realistic volatility term structure similar

to the structure observed in the market (Andersen and Buffum, 2002).

$$\lambda(t, S) = a(t)(\frac{S(0)}{S})^p \tag{2.6}$$

$$\sigma(t, S) = b(t) \tag{2.7}$$

Note that the p in Equation 2.6 is not the same as $p(s, y)$ in the Fokker-Planck equation. This p is the ratio between the credit spread volatility and equity volatility, and has been found to be between 1.2 and 2 for Japanese bonds rated BB+ and below (Muromachi, 1999). As presented in Andersen and Buffum (2002) we solve the Fokker-Planck equation, also known as the forward Kolmogorov equation, for a diffusion process with jumps. The Fokker-Planck equation describes the time-evolution of the discounted probability distribution, $p(s, y)$, of log stock prices for a jump-diffusion process is as follows:

$$-\frac{\partial p}{\partial s} - \frac{\partial}{\partial y}(r - q + \lambda - \frac{1}{2}\sigma^2)p + \frac{1}{2}\frac{\partial^2}{\partial y^2}\sigma^2 p = (r + \lambda)p \tag{2.8}$$

where s is the timestep and y the is natural logarithm of the stock price. Solving the equation yields the shape shown in Figure 2.2.

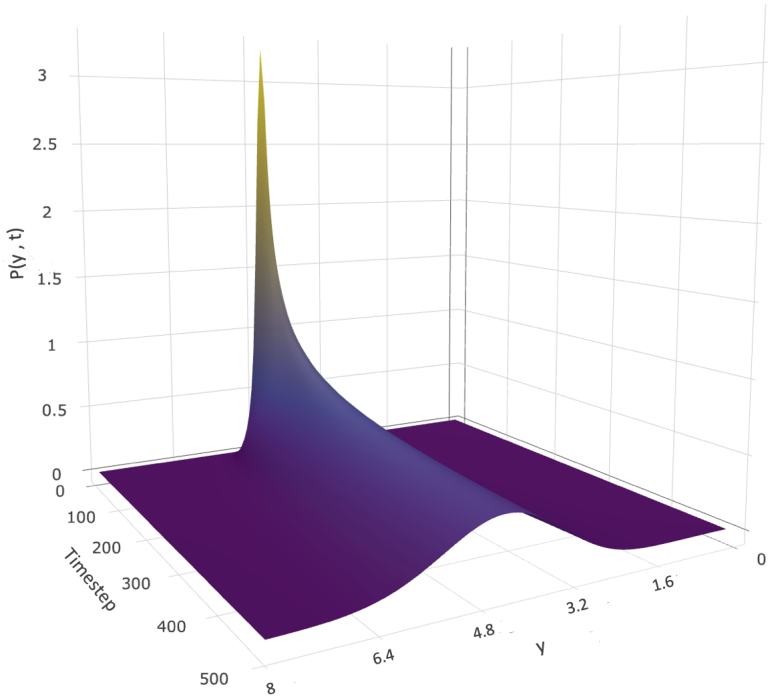

Figure 2.2: Time-evolution of probability distribution of stock prices. y is the natural log of the stock price.

As initial condition we use the dirac delta function, which is $\frac{1}{dy}$ at today's stock price and zero for all other stock prices, and hence the initial probability distribution sums

to 1. Note that the right-hand side of Equation 2.8 is non-zero, which means that the probability space is discounted in each time step, i.e. the probability density will no longer sum to one. This is also done by Andersen and Buffum (2002) and is to avoid discounting when computing call and zero-coupon bond prices, which is done with the following two equations:

$$C(T_i, K_i) \approx \Delta y \sum_{y_0 + j\Delta y > ln(K_i)} p(T_i, y_0 + j\Delta y)(e^{y_0 + j\Delta y} - K_i) \tag{2.9}$$

$$B(0, T_i) \approx \Delta y \sum_{j>=0} p(T_i, y_0 + j\Delta y) \tag{2.10}$$

Here $p(T_i, y_0 + j\delta y)$ is the discounted probability of a given log stock price at timestep T_i and K is the strike price of the call option to be matched. With the above equations we can find the value of a call option or of a zero-coupon bond of a stock with the given price dynamics at any maturity, which enables us to match the implied volatility and credit spread of the model to the implied volatility and credit spread of traded derivatives in the market place at different maturities. We are hence able to capture the term structures of volatility and risk assessed by the market.

As zero-coupon corporate debt is rarely, if ever, issued, we imply the credit spread using credit default swaps (CDS) instead, as suggested by Andersen and Buffum (2002). CDS' are bought as insurance against default events of a company, so the price (which is in basis points on 100$ of bond value) should on average equal the credit spread of the bond to eliminate arbitrage opportunities. Differences between the price of the CDS and the credit spread of a bond is called *basis*, and can arise due to differences in the documentation of the bond and the CDS, debt buybacks, restructurings and changes in credit ratings. For instance could a bond with an investor's put provision trade at a lower credit spread than that implied by the CDS, i.e. there is positive basis, due to the insurance inherent in the bond that is not covered in the CDS documentation. Due to data limitations we assume zero basis and use CDS prices as a direct measure of credit spread.

In order to properly calibrate the model to capture the volatility term structure and time-dependent credit spread we solve the Fokker-Planck equation and compute at-the-money

call values and zero-coupon bond values with Equation 2.9 and Equation 2.10 for different values of $a(t)$ and $b(t)$ until they match market prices for selected maturities. To do this efficiently we employ a Newton-Raphson iterative method in the manner presented by Andersen and Buffum (2002). First we freeze $a(t)$ and solve for $b(t)$ by matching option values to market. Then we freeze $b(t)$ and solve for $a(t)$ by matching the zero-coupon bond value with the one implied from the CDS spread in the market. We repeat this process until both call options and zero-coupon bonds deviate less than 1% from their respective market prices.

This calibration gives the forward outlook of the market on volatility and credit risk and will only be valid to compute the present day convertible bond price. In this thesis we seek to compute CB values over a range of times going backward, which would require that we have both historical option and CDS data. As this data is very difficult to obtain without purchasing it, we assume a constant volatility term structure that we vertically shift when volatility level changes. Hence, when backtesting on historical data we assume that the volatility outlook is the same at any point in time except for a vertical shift according to the volatility computed with the GARCH model. As for the credit spread we assume the term structure of risk to be constant over the whole period rather than vertically shift it when CDS rates change. The reason is that the CDS data collected from DataGrapple is very volatile and is from low trading volumes. Also, the data is only free to view, but has to be purchased in order to download it.

The GARCH model we use is a simple GARCH(1,1) model, which estimates the current conditional variance by a weighted average of the conditional variance and squared return one day earlier.

$$\sigma_t^2 = \omega + \alpha\epsilon_{t-1}^2 + \beta\sigma_{t-1}^2,\ \epsilon | I_{t-1}\ N(0, \sigma_t^2) \tag{2.11}$$

The GARCH parameters ω, α and β are found by maximizing the log likelihood function in Equation 2.12 over the desired range of returns.

$$lnL(\theta) = \frac{-1}{2}\Sigma_{t=1}^{T}\left(ln(\sigma_t^2) + (\frac{\epsilon_t}{\sigma_t})^2\right) \tag{2.12}$$

Combining GARCH and Fokker-Planck we are thus able to compute volatility and credit spread estimates over the remaining time to maturity of the convertible bond, for any point in time during the selected trading period.

2.3 Numerical considerations

Both the stochastic PDEs of the AFV model and the Fokker-Planck equation are parabolic PDEs, which means that both convergence and stability are necessary properties of the solution method. In order for explicit finite difference methods to be stable, it is necessary that $r = \frac{dt}{dy^2} <= \frac{1}{2}$. Since Crank-Nicolson averages both implicit and explicit methods, it is not restricted by this time to spacial resolution ratio, and it is unconditionally stable for many common parabolic PDEs (Kreyszig, 2010). We find, however, that we need r to be 1 or less to avoid oscillations in the solution.

When performing the calibration we experience that a regular discretization of the Fokker-Planck, as described in Appendix C, results in a loss of probability (before probabilities are discounted) at each timestep so that the sum under the probability distribution is no longer 1. For high values of p such as 2 in the exponent in Equation 2.6 the loss over a 5 year period can be as large as 30%! The result is a significant underestimation of the discount rate $a(t)$ which in turn yields an overestimation in the CB prices. We find that using *upwind discretization* as explained in Appendix D, which is a conservative method used for convection-diffusion problems in computational fluid dynamics, this loss of probability is virtually eliminated.

Chapter 3

Data

Based on the requirements of the AFV model we need the underlying companies to have a liquid market for both options and CDS-contracts, and the CBs in themselves need to be frequently traded. Obtaining trading data for these instruments is difficult and is best done with paid-subscription services such as Bloomberg. Lacking access to such services, our analysis is limited to data that is publicly available.

3.1 Data sources

Wharton Reasearch Data Services (WRDS) provides researchers with access to over 350 terabytes of data across multiple disciplines including accounting, banking, economics, ESG, finance, healthcare, insurance, marketing, and statistics. From WRDS we gather an overview of issued convertible bonds as well as bond trading data up until 2018-12-31, which lays the basis for the analysis. We further retrieve trading data up until 2019-04-23 from markets.businessinsider.com for the selected bonds.

DataGrapple is a database of daily CDS data for maturities 1, 3, 5, 7, and 10 years from 2006-01-03 until the present time from the credit derivatives database of Hellebore Capital. In the U.S. market it has data for 132 high yield companies and 127 investment grade companies from basic materials, communications, consumer, energy, financial, industrial, technology and utilities sectors.

We compute volatility estimates by running a GARCH model on stock returns from 2015-01-01 to 2019-04-23 with the stock prices scraped from Yahoo Finance. The option data is scraped from option chains on nasdaq.com, while the terms of the convertible bonds are from the U.S. Securities and Exchange Commission(SEC).

3.2 Bond selection

In order to be able to perform the analysis we need stock closing prices, call option data, CDS data and historical convertible bond prices. The lack of historical option data excludes all convertible bonds that are not currently traded from the sample.

From WRDS we obtain a dataset of historical trading data on 1,018 different convertible securities with maturities later than 2019-04-23. Further, we remove all securities that are not characterized as "FXPV", meaning "fixed coupon plain vanilla", leaving 746 potential convertible bonds. Filtering for convertible bonds issued by companies included in the DataGrapple CDS dataset leaves 29 possible convertible bonds for analysis. Closer scrutiny of the bond sample reveals that 5 have been redeemed and are no longer trading, 2 were never actually issued, 3 are issued by private companies, 13 have put and/or call features or special conversion criteria. Also, we could not find documentation for 3 of the convertible notes, leaving 3 convertible bonds suitable for analysis. These three bonds are the TSLA2022 2.375%, RIG2023 0.5% and STAR2022 3.125%. As there has been a change in conversion ratio in Nov 2018 of the STAR2022 3.125%, and since we lack convertible bond trading data after 12/12/2018, we omit it from the sample, leaving just two convertible bonds: TSLA2022 2.375% and RIG2023 0.5%.

Table 3.1: Convertible Bond Sample

Company name	Ticker	Coupon	Issue date	Maturity	Issuer vol.[1]	ISIN
Tesla Inc.	TSLA	2.375%	03/16/'17	03/15/'22	977,500	US88160RAD35
Transocean Inc.	RIG	0.5%	01/30/'18	01/30/'23	561,440	US893830BJ77

[1] In $1000.

Chapter 4

Results

The first part of this chapter presents the features of each convertible bond and explains how we obtain the price, delta and gamma results. We then calculate the price surface for each bond at each of the 305 trading days between 2018-02-01 and 2019-04-23. We choose this period because RIG2022 was issued 2018-01-30, hence it was not traded before this date. The last date in the selected period, 2018-04-23, was the last trading day before we scraped the data. Note that the price we find at every trading day is the dirty price, whereas the prices we compare to are clean prices. The difference is that dirty prices include accrued coupons whereas clean prices have subtracted accrued coupons to remove the sawtooth effect on prices. Thus, some deviation will be caused by accrued coupons, but will at most be 0.25% for RIG and 1.1875% for TSLA as the coupons are paid semiannually. To extract the delta and gamma from the price surfaces at a specific time we use the central differences method, as shown in Equation 4.1 and 4.2:

$$\Delta_i = \frac{P_{i+1} - P_{i-1}}{2 \cdot cr \cdot \Delta S} \tag{4.1}$$

$$\gamma_i = \frac{P_{i+1} - 2P_i + P_{i-1}}{cr \cdot (\Delta S)^2} \tag{4.2}$$

where i refers to stock price i, P_i is the price of the CB at stock price i, cr the conversion ratio of the CB, and ΔS the step between stock prices on the time-stock price grid.

In section 4.1 and 4.2 we present the bonds selected in this paper and the resulting prices, deltas and gammas over the backtesting period. In Section 4.3 we present the analysis of the delta hedging performance of the model.

4.1 Bond Case 1: TSLA

Tesla, Inc.[ticker: TSLA] is an American automotive and energy company based in Palo Alto, California. The company specializes in electric car manufacturing and, through its SolarCity subsidiary, solar panel manufacturing.

The first bond we analyze is the $977.50m convertible bond by Tesla Inc. maturing in 2022 with the features described in Table 4.1.

Table 4.1: CB features TSLA2022

CUSIP	88160RAD3
ISIN	US88160RAD35
Issue date	16 March 2017
Maturity	15 March 2022
Coupon	2.375% p.a. semiannual payment
Conversion ratio	3.0534 per $1,000
Face Value	$977,500,000
Call feature	No
Put feature	No

We run the aforementioned GARCH-model on adjusted close prices scraped from Yahoo Finance to obtain time-dependent volatility estimates, as seen in Figure 4.1.

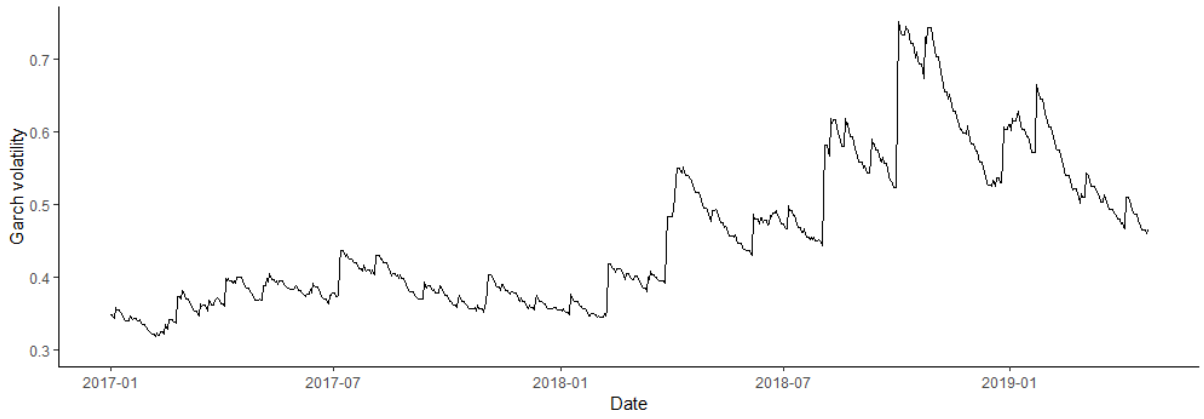

Figure 4.1: TSLA Volatility

We also collect European call option prices on TSLA with maturities from 3 days forward to 633 days forward by scraping from NASDAQ, these are shown in Table 4.2

Table 4.2: European call option prices for TSLA as of market closing 2019-04-23, s=263.9

Date\Strike	260	262.5	265	267.5	270	272.5	275	277.5	280
2019-04-26	13.19	11.75	10.30	9.05	8.00	6.90	5.90	5.07	4.23
2019-05-03	15.50	13.35	12.80	11.20	10.10	8.80	8.30	7.45	6.60
2019-05-10	16.82	16.02	14.70	13.09	12.29	11.18	10.15	8.82	8.00
2019-05-17	18.91	16.91	16.25	15.00	13.77	13.15	11.55	10.32	9.77
2019-05-24	20.40	18.50	17.50	15.55	15.10	14.80	12.81	12.60	11.30
2019-05-31	21.45	20.21	18.36	17.80	16.27	15.46	14.05	13.25	11.50
2019-06-21	24.70		22.20		19.90		17.73		15.40
2019-07-19	28.98		26.38		24.43		21.65		19.90
2019-08-16	34.50		31.85		29.25		27.20		24.22
2019-09-20	38.00		35.20		32.73		30.20		27.72
2019-11-15	43.70		41.94		39.90		36.85		34.86
2019-12-20	46.70		44.82		43.01				
2020-01-17	48.99		46.48		43.94		42.00		40.30
2020-06-19	60.50				56.25				52.30
2021-01-15	72.30		70.00		66.65		65.25		63.65

The CDS data is gathered from DataGrapple and shown in Table 4.3.

We estimate the p from Equation 2.6 to be approx. 6. This is very high and would implicate that a 50% decline in share price would yield a 64 times increase in credit spread. We find this to unrealistic and note that a p of 2 is the highest value found by Muromachi (1999). This would implicate that a 50% drop in the share price would yield a 4 times increase in credit spread, which we find to be a more reasonable number. To find the optimal value of p we run the complete pricing model over a range of 305 trading days and select the p that yields the lowest average error to the observed market prices. For TSLA we find $p = 2.5$ to yield reasonable results. A higher value of p would be preferable but oscillations start to occur already at 2.5 for some dates, on which we use extrapolation

Table 4.3: CDS spreads for TSLA as of market closing 2019-04-23

Date	Spread (bps)
2020-04-23	439
2021-04-23	
2022-04-23	529
2023-04-23	
2024-04-23	531
2025-04-23	
2026-04-23	511
2027-04-23	
2028-04-23	
2029-04-23	434

from lower values of p. The stability can be increased by reducing the resolution in stock prices, but this introduces inaccuracy due to larger price steps.

By solving the Fokker-Planck equation described in Section 2.2, and adjusting the input parameters $a(t)$ and $b(t)$ such that the model's zero-coupon bond values and call option values match market CDS and option data, we get $a(t)$ and $b(t)$ as shown in Figure 4.2 and Figure 4.3, respectively. The calibrated $b(t)$ fits closely to the implied volatility, and one can clearly observe that the shape is well captured. The distance between the two curves is dependent on p from Equation 2.6. The higher the p, the higher will the curve for $b(t)$ lie. To understand how $a(t)$ and $b(t)$ interact, we refer to Figure E.3 in the Appendix, which is from Andersen and Buffum (2002). Note that the figure is made to fit constant term structures whereas our calibration is fit to real, non-linear term structures.

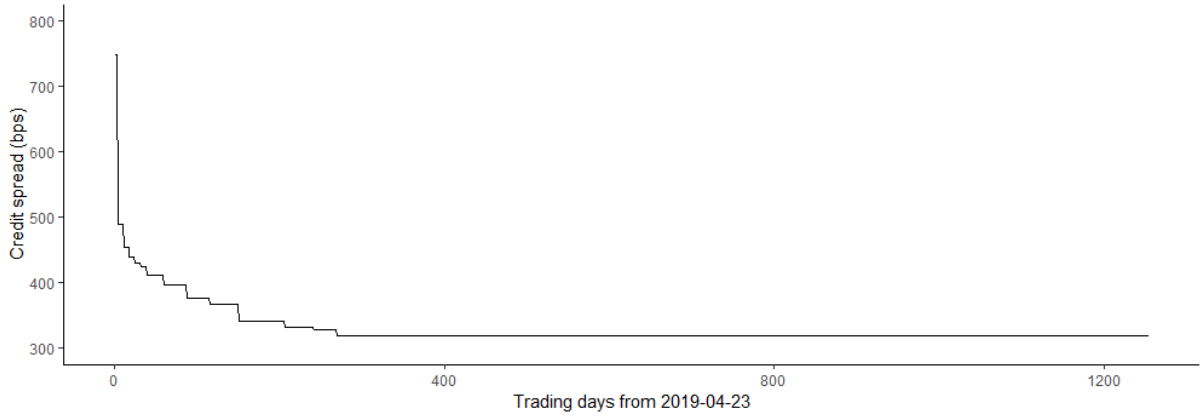

Figure 4.2: TSLA calibrated a(t)

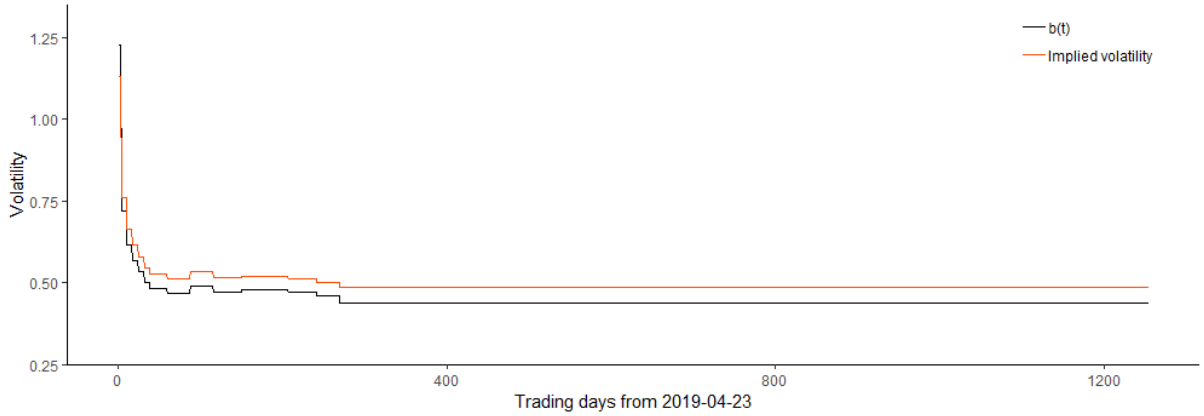

Figure 4.3: TSLA Volatility termstructure, b(t)

We infer the recovery rate in case of default, R, from CDS spreads and the probability of default (PD) from DataGrapple through Equation 4.3 which yields R to be 0.451 with the spread being 439 bps and the PD being 8%. As the CDS spread is likely to include a small profit premium we use $R = 0.5$.

$$Spread_{CDS} = PD \cdot [Loss|Default] \implies R = 1 - [Loss|Default] = 1 - \frac{Spread_{CDS}}{PD} \quad (4.3)$$

Finally, we run the AFV model to compute a price surface of the convertible bond price at all stock prices and times from 2019-04-23 until maturity. We obtain a price of 108.01 from the price surface, whereas the market price on 2019-04-23 was 107.11. The model thus overestimates the market price by 0.8% at this stock price and point in time. The delta is 0.6464, compared to 0.5907 in the Tsiveriotis-Fernandes model ("TF model") (Tsiveriotis and Fernandes, 1998) and 0.5730 in the Goldman Sachs model ("GS model")

(GoldmanSachs, 1994). The delta from AFV is slightly higher due to the modeling of default dynamics with $R = 0.5$ and $p = 2.5$, but all models indicate that a delta around 0.6 is reasonable.

We further run the model over the 305 trading days between 2018-02-01 and 2019-04-23, creating 305 price surfaces and get prices, deltas and gammas on each trading day. The price comparison is presented in Figure 4.4 and shows that the market prices lag the model prices by 1 day. Correcting for this the prices have a correlation of 0.920 and an average error of 3.025%, i.e. an overpricing compared to the market.

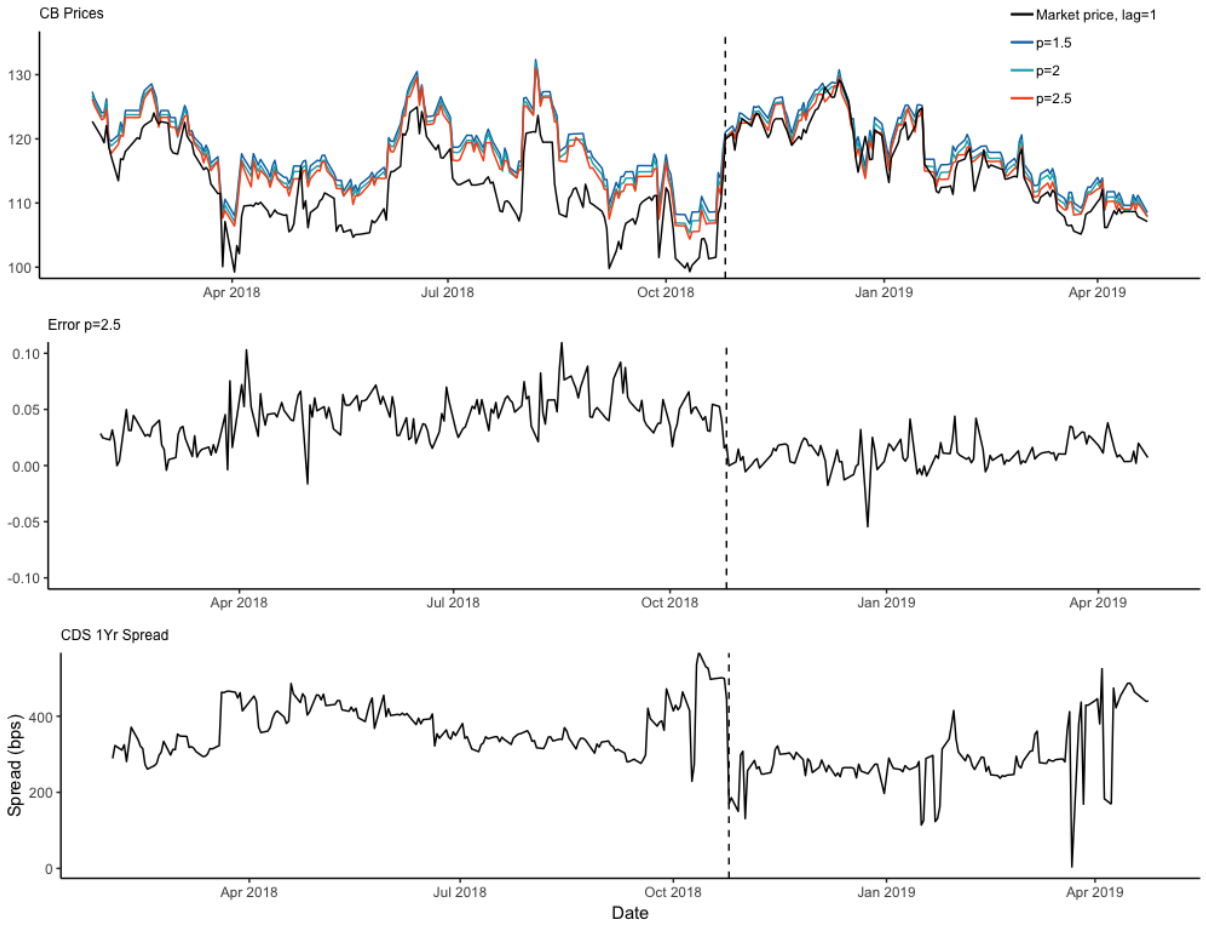

Figure 4.4: TSLA Price Comparison

We observe that there is a structural change in the error around 2018-10-25. Between this date and 2019-04-23, the most recent date in our sample, the average error is only 0.93%, indicating little to no mispricing. This increases to 4.35% over the rest of the sample. The reason is a change in the complete yield curve which our model does not capture. We only calibrate 633 days forward, which is when we have option data, and hence do not

capture changes in the 3, 5, 7 and 10 year CDS-spreads. Also, we do not take into account historical changes in the credit spreads, but only calibrate the risk structure with data from 2019-04-23, as explained in Section 2.2. The rates of all maturities, and especially longer rates, decrease significantly between 2018-10-23 and 2018-11-08, which means that the discount rates used in the market were higher prior to 2018-10-23 than what we have calibrated in this time period. Hence, we get higher prices than the market in this time period.

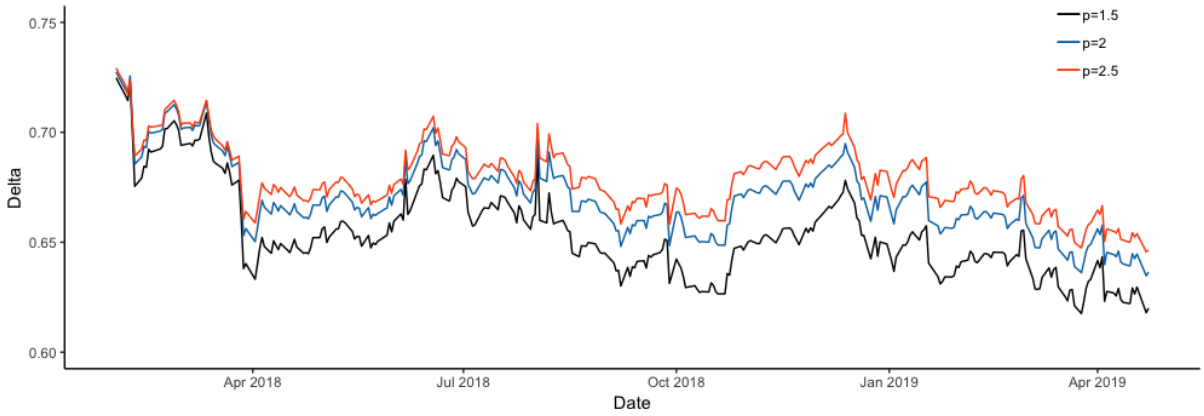

Figure 4.5: The delta for TSLA for p = 1.5, 2 and 2.5

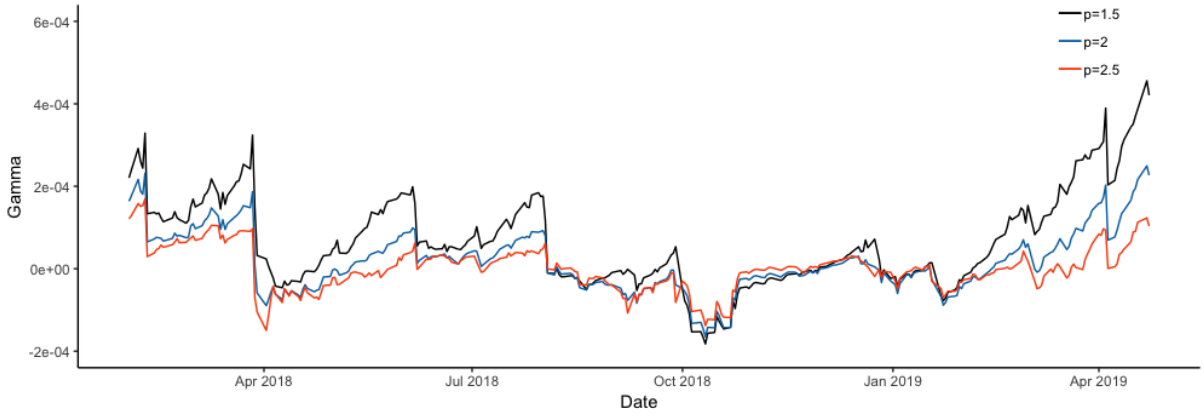

Figure 4.6: The gamma for TSLA for p = 1.5, 2 and 2.5

As seen in Figure 4.4 the value of p has little effect on prices. The differences are much more pronounced in the delta and gamma, as shown in Figure 4.5 and Figure 4.6 respectively. From a convertible arbitrage standpoint it is interesting to assess the robustness of a convertible arbitrage strategy to the value of different model parameters to gauge how the strategy is affected by estimation error.

4.2 Bond Case 2: RIG

Transocean Ltd.[ticker: RIG] is the world's 2nd largest offshore drilling contractor and is based in Vernier, Switzerland. The company has offices in 20 countries, including Switzerland, Canada, United States, Norway, Scotland, India, Brazil, Singapore, Indonesia and Malaysia.

The second bond is the $561.44m convertible bond by Transocean Inc. maturing in 2023 with the features described in Table 4.4:

Table 4.4: CB features RIG2023

CUSIP	893830BJ7
ISIN	US893830BJ77
Issue date	30 January 2018
Maturity	30 January 2023
Coupon	0.5% p.a. semiannual payment
Conversion ratio	97.29756 per $1,000
Face Value	$561,440,000
Call feature	No
Put feature	No

We run the GARCH-model and compute the time-dependent volatility estimates shown in Figure 4.7.

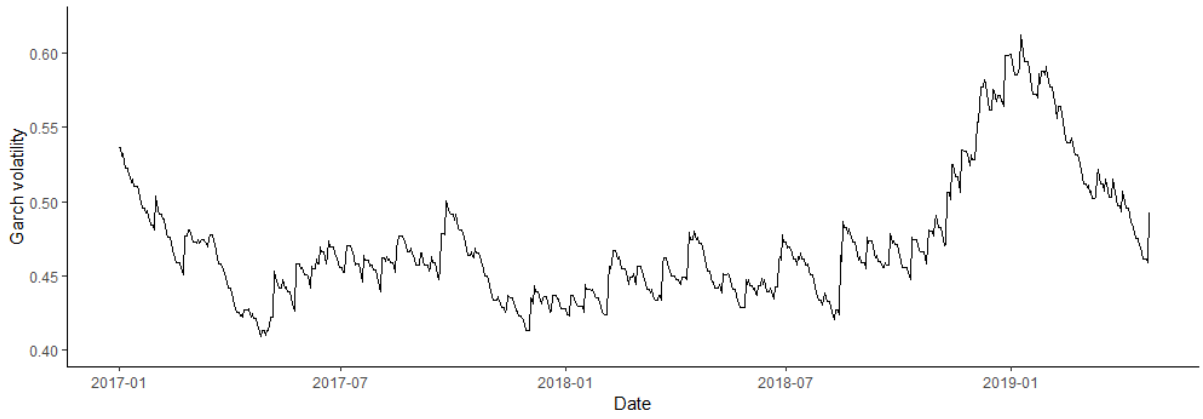

Figure 4.7: RIG Volatility

Table 4.5 displays the retrieved European call option prices on RIG with maturities from 3 days forward to 633 days forward from NASDAQ.

Table 4.5: European call option prices for RIG as of market closing 2019-04-23, s=9.65

Date\Strike	10	10.5	9	9.5
2019-04-26	0.06	0.01	0.67	0.25
2019-05-03	0.20	0.08	0.77	0.40
2019-05-10	0.26	0.13	0.88	0.54
2019-05-17	0.34	0.21	0.89	0.56
2019-05-24	0.41	0.21	0.91	0.65
2019-05-31	0.45	0.27	0.88	0.66
2019-06-21	0.55		1.06	
2019-08-16	0.87		1.36	
2019-11-15	1.16		1.77	
2020-01-17	1.44		1.82	
2021-01-15	2.47			

The CDS data is gathered from DataGrapple and shown in Table 4.6.

Table 4.6: CDS spreads for RIG as of market closing 2019-04-23

Date	Spread (bps)
2020-04-23	78
2021-04-23	
2022-04-23	258
2023-04-23	
2024-04-23	425
2025-04-23	
2026-04-23	588
2027-04-23	
2028-04-23	
2029-04-23	613

We estimate the p from Equation 2.6 to be approx. 12, or almost double what we found p to be for TSLA. We find this to be unrealistically high and is caused by too high estimated volatility for the CDS price, which in turn is a result of low trading volume in the instrument. Nonetheless, the theoretical calculated p indicates that the p should be higher than 2. To find the optimal value of p we run the complete pricing model over the range of the 305 trading days and select the value that yields the lowest average error to the observed market prices. For RIG we find $p = 3.5$ to yield reasonable results. This is the highest p we could run without having any computational disturbances and instability. As for TSLA the stability can be increased by reducing the resolution in stock prices, but this introduces inaccuracy due to larger price steps.

By calibration with the Fokker-Planck equation, we get the following $a(t)$ and $b(t)$, shown in Figure 4.8 and Figure 4.9:

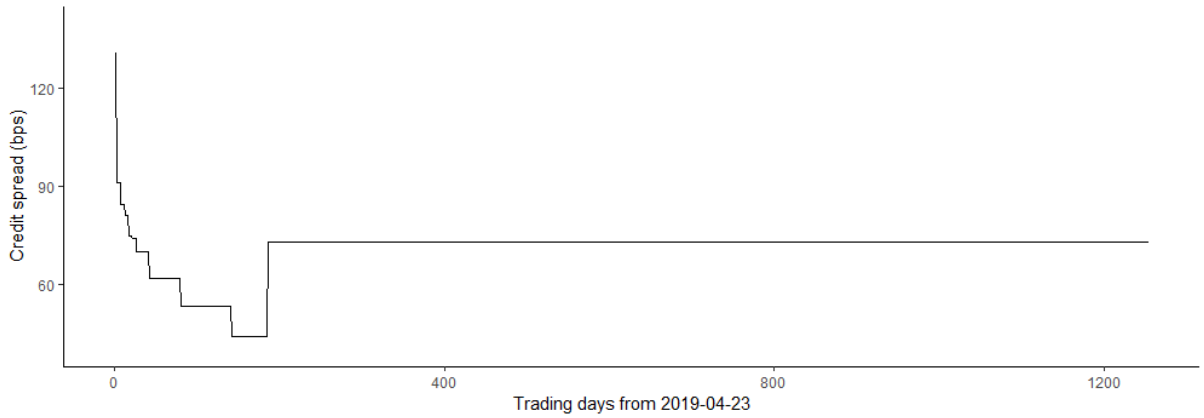

Figure 4.8: RIG calibrated a(t)

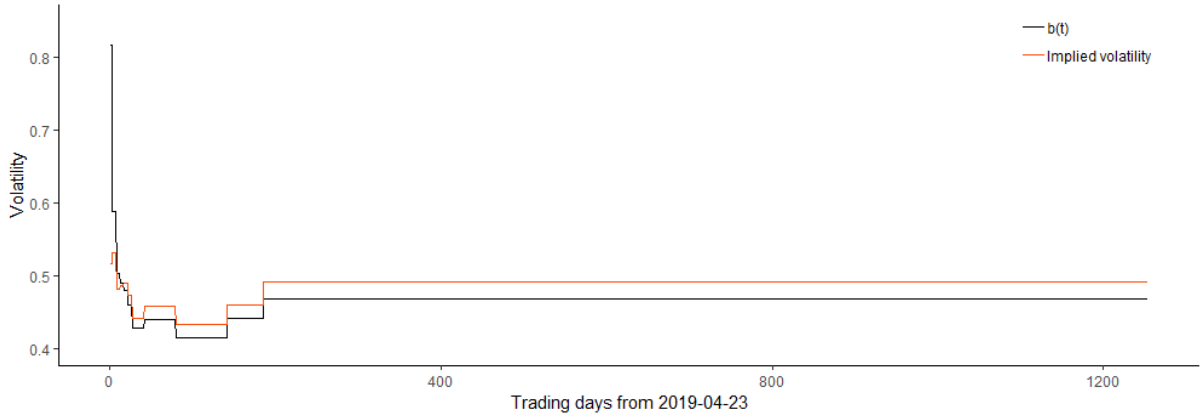

Figure 4.9: RIG Volatility term structure, b(t)

In the same manner as for TSLA, we obtain an estimate of recovery rate in case of default, R, using Equation 4.3. With the $\text{Spread}_{\text{CDS}}$ being 78 bps and the PD being 2% we estimate R to be 0.6.

Finally, we run the AFV model to compute a price surface of the convertible bond price at all stock prices and times from 2019-04-23 until maturity. From the price surface we obtain a theoretical price of 119.51, whereas the market price was 110.60. At this point in time the model overestimates the market price by 8.1%. The delta theoretical delta is found to be 0.7496, whereas the delta in the TF model and GS model is 0.7203 and 0.6889 respectively, which indicates that the delta should lie around 0.7-0.75.

We further run the model backwards over the 305 trading days from 2018-02-01 to 2019-04-23, creating 305 price surfaces and get the corresponding price, delta and gamma to the stock price at each trading day. The prices obtained, as well as the deviations from the market price, are shown in Figure 4.10. The deltas and the gammas are shown in Figure 4.11 and 4.12. As for TSLA the market price lags the model price by 1 day.

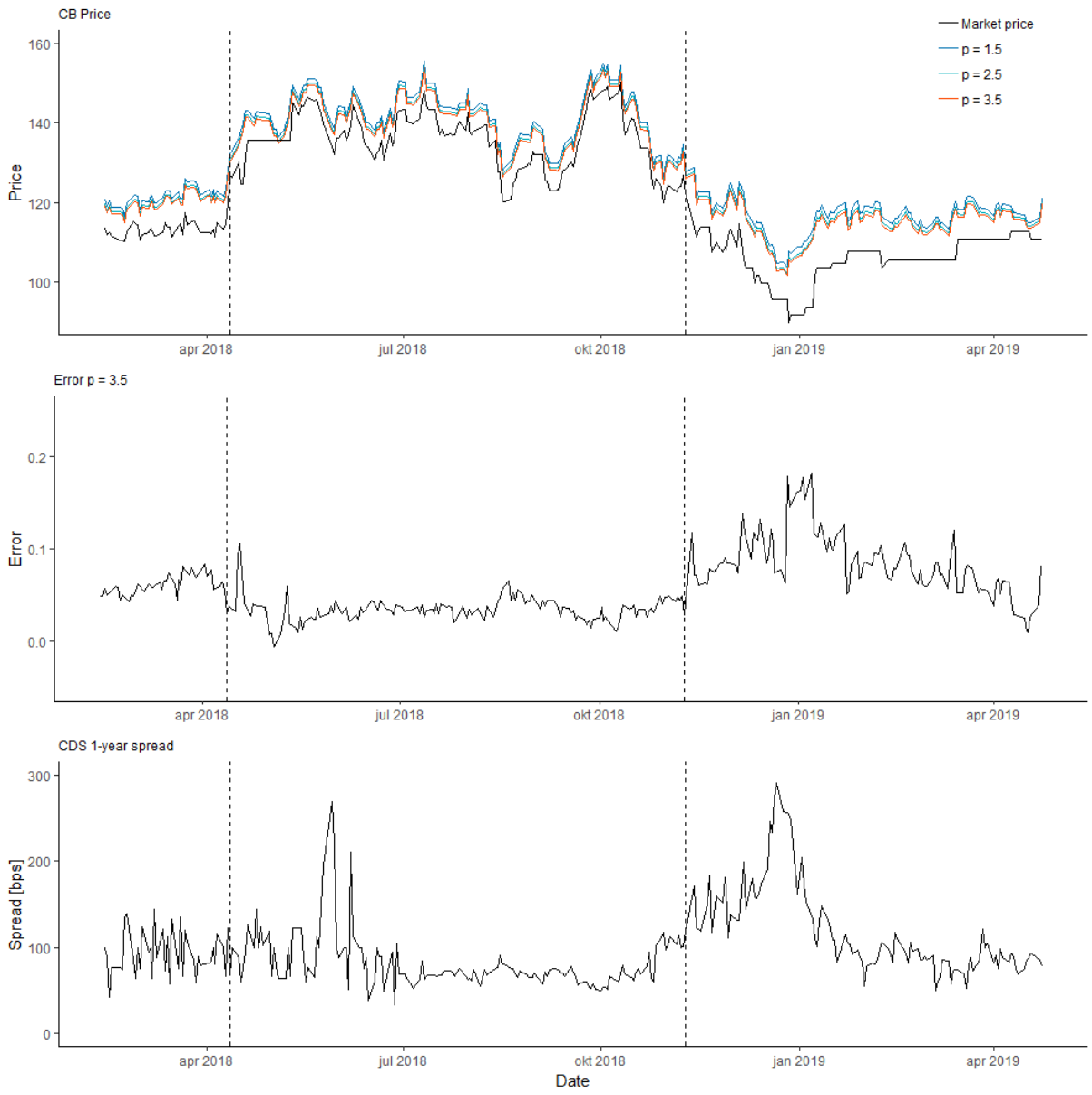

Figure 4.10: RIG Price Comparison, with the period 2018-04-11 to 2018-11-08 within the dashed markers.

Correcting for the one day lag, the prices have a correlation of 0.662 and an average error of 5.6%. However, if we look at the period from 2018-04-11 to 2018-11-09 the correlation increases to 0.931 and the average error falls to 3.4%. In this period the CB trades in-the-money, where the implied credit spread and volatility are low and the stock price is high. When the stock price drops, volatility rises and the credit spread increases, the error also increases. This implies that the model performs better when the CB is in-the-money than at- or out-of-the-money.

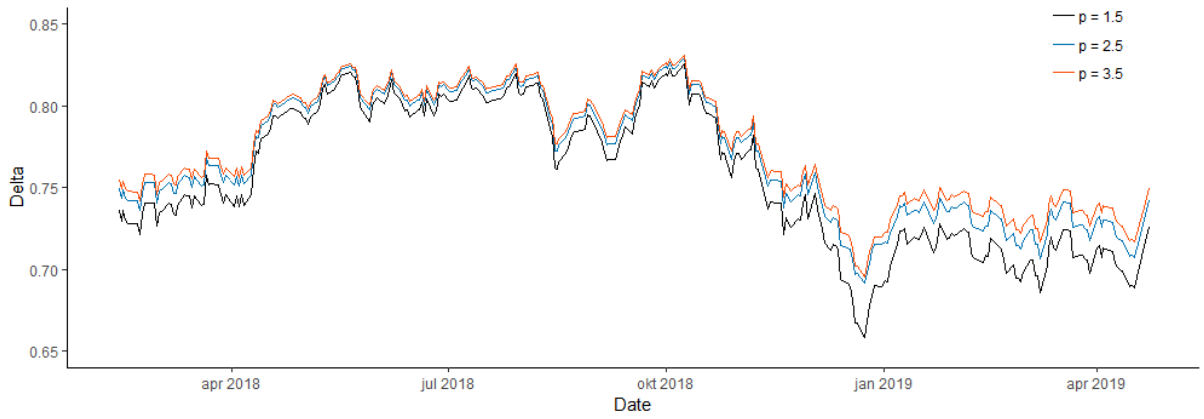

Figure 4.11: The delta for RIG with p = 1.5, 2.5 and 3.5

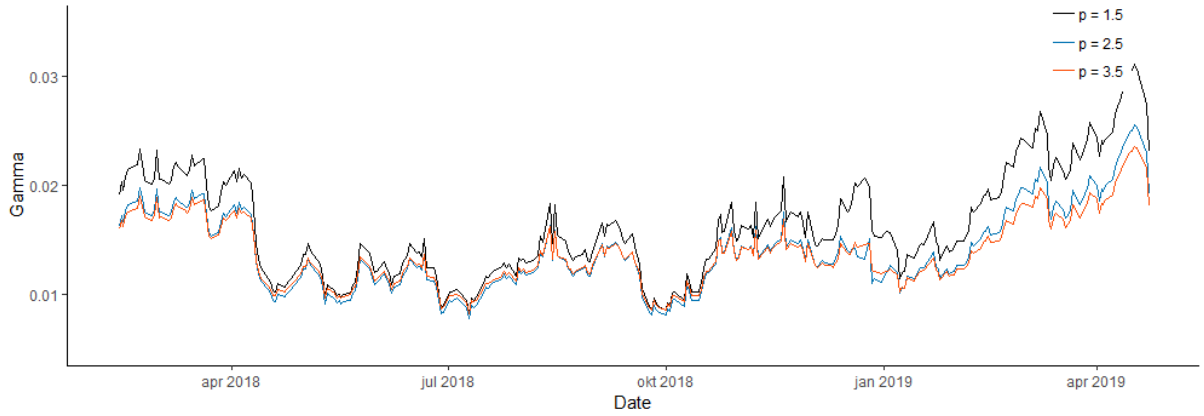

Figure 4.12: The gamma for RIG with p = 1.5, 2.5 and 3.5

RIG displays the same pattern as TSLA, Figure 4.10 shows that p has little effect on prices. The differences are more pronounced in the delta and gamma, as shown in Figure 4.11 and Figure 4.12 respectively. We observe that the biggest differences in delta and gamma is where the price is lowest, which is where delta is lowest and the gamma is highest. This is where the CB trades at- or out-of-the-money. The observed effect is shown in Figure E.1a and E.2a, where p has the most influence where the CB trades out-of-the-money .

4.3 Delta hedging with the AFV model

As explained in Section 1 a convertible arbitrage strategy consists of a long position in the convertible bond and a short position in the underlying stock. To determine the size of the short position one must assess the delta of the convertible bond. As shown in the previous section the delta is more sensitive to p than the price is, and is thus a risk factor to convertible bond arbitrageurs. We also find that the delta is most sensitive to the assumed recovery rate, R, as illustrated in Figure E.2b, and to the volatility, as can be seen in Figure E.2c.

In Section 4.1 and Section 4.2 we mentioned that there is a 1 day time lag between the market prices and those obtained from the model. The reason is that the stocks are listed in the US whereas the bonds trade in Europe, hence the market prices for the convertible will lag behind the stock prices. This presents an issue for daily hedging, and will expose the arbitrageur to intraday risk. However, assessment of this risk is beyond the scope of this thesis, and in order to evaluate the effectiveness of the delta hedge we simply lag the stock returns to match the returns of the convertible bonds as if they were traded simultaneously.

We define hedging error, ϵ_t, in the same manner as Ammann and Seiz (2006), but with lagged stock returns, as shown in Equation 4.4:

$$\epsilon_t = \frac{(V_t - V_{t-1}) - \delta_{t-1}(S_{t-1} - S_{t-2})}{V_t} \tag{4.4}$$

In Figure 4.13 we demonstrate that although the AFV model fits closely on price, the delta does not work for delta hedging the TSLA CB. A linear regression of CB returns on lagged stock returns yields a slope of 0.4248, which should indicate the level of the average delta. The AFV model, however, yields an average delta of 0.6790, which is substantially higher and implies that the market prices of the CB are less sensitive to changes in the underlying stock price than the AFV model suggests, suggestions which were in line with both the TF and GS models. We find that a tuning factor, which we define as $f_\epsilon = \frac{\Delta_{market}}{\Delta_{model}} = 0.51507$, minimizes the squared correlation of the mid 80% quantile of

stock returns, which consists of daily stock returns in the range $[-3.577\%, 3.431\%]$. The quantile correlations with the underlying stock returns of the CB, original delta hedged portfolio and modified delta hedged portfolio, respectively, are shown in Table 4.7. From the negative correlations for the delta hedged portfolio in the table we clearly see that the short position, which is negatively correlated with the stock, and hence the delta, is too large. We also see that by modifying the delta by f_ϵ the correlation is virtually zero on 80% of the trading days, indicating a good delta hedge. The positive correlations in the tails are to be expected in a delta hedged portfolio and should be due to the convexity of the CB.

Table 4.7: TSLA quantile correlations

Quantile	Bottom 10%	Mid 80%	Top 10%	Total correlation
Unhedged	0.5497	0.4721	0.6144	0.6961
Model delta	-0.0884	-0.4369	-0.1703	-0.5201
Modified delta	0.2525	$1.07 \cdot 10^{-16}$	0.2701	0.1392

As seen in Figure 4.13a the hedging error is reduced on most days, and especially on December 25th 2018. 4.13b and 4.13c illustrate that the hedging error is much more centered around zero, and there are more trading days with lower errors. 4.13d and 4.13e show that a second order polynomial provides a much better fit to explain the residual risk after delta hedging when the modified deltas are employed. This demonstrates that a substantial part of the tail correlation from Table 4.7 is indeed due to the convexity, or gamma, of the CB.

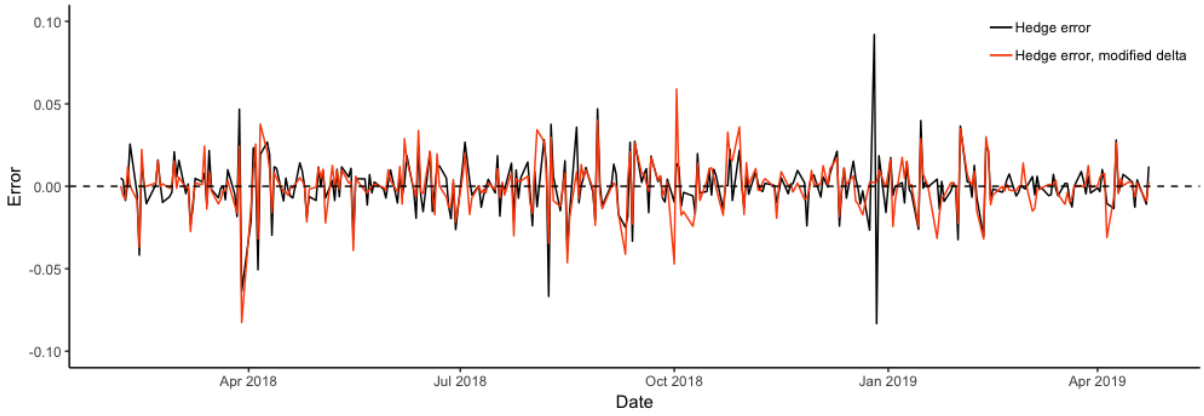

(a)

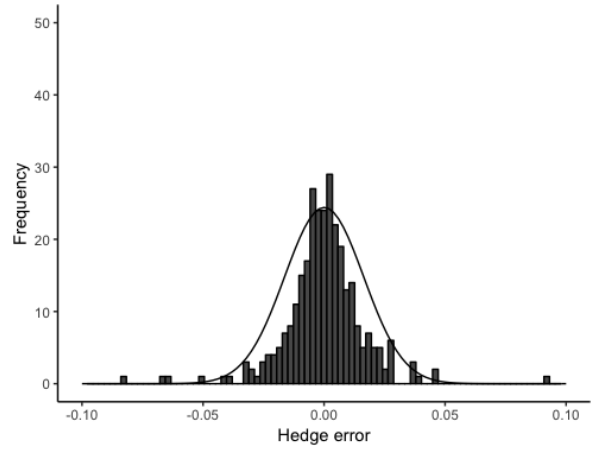

(b)

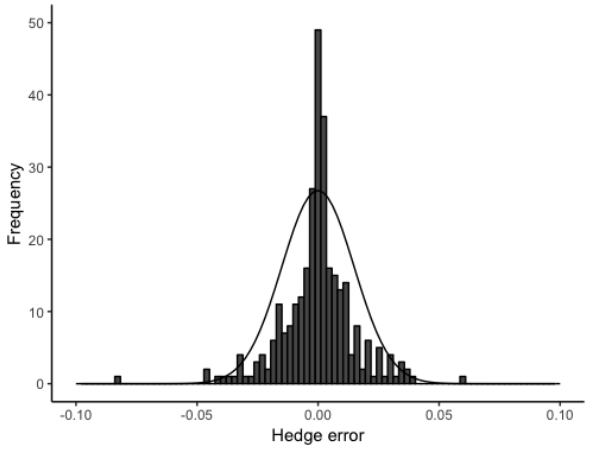

(c)

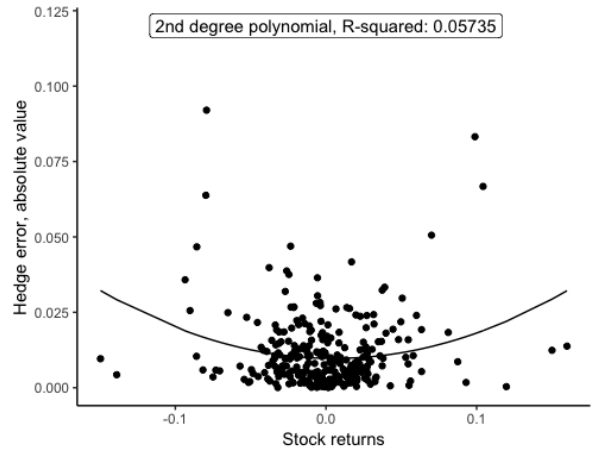

(d)

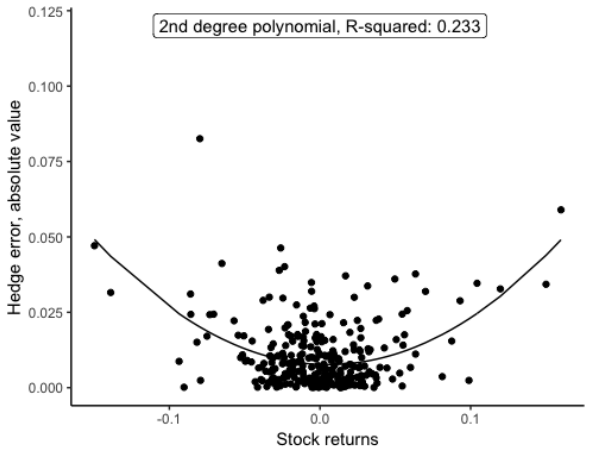

(e)

Figure 4.13: Hedging performance for TSLA. (a) Hedging error over time. (b) Hedge error histogram before correction, N($\mu = 2.731e-05$,$\sigma = 0.0163$) superimposed. (c) Hedge error histogram after correction, N($\mu = -3.984e-05$,$\sigma = 0.0149$) superimposed. (d) Hedge error in absolute value on stock returns. (e) Hedge error in absolute value on stock returns after correction factor

For RIG the mid 80% quantile is the range $[-3.66\%, 3.55\%]$. Minimizing the squared correlation between the hedged portfolio and stock returns in the mid 80% quantile, we obtain a tuning factor, f_ϵ, of 0.746841. In Table 4.8 we see the effect the tuning factor has on the hedged portfolio, particularly that the correlation in the mid 80% quantile goes from -0.2444 with the original delta to $7.4 \cdot 10^{-8}$ after applying the tuning factor. The total correlation is -0.0960 using the tuning factor, compared to -0.3812 using the original model delta.

Table 4.8: RIG quantile correlations

Quantile	Bottom 10%	Mid 80%	Top 10%	Total correlation
Unhedged	0.2885	0.6158	-0.0723	0.6621
Model delta	-0.1860	-0.2444	-0.3775	-0.3812
Modified delta	-0.0686	$7.4 \cdot 10^{-8}$	-0.3109	-0.0960

Figure 4.14 displays how the tuning factor affects the hedging error for RIG. Figure 4.14a shows how the tuning factor dampens the error where the model is least accurate, but increases the error where the model delta is most accurate. 4.14d and 4.14e exhibit that when applying the modifying factor, f_ϵ, to the delta, the second degree polynomial has more explaining power than just using the model delta, increasing the R^2 from 0.2479 to 0.3329. Looking at the histograms in 4.14b and 4.14c the effect of a modifying factor seems to not have as good effect for RIG as it had for TSLA. This is due to RIG having different structural periods, the period from 2018-04-23 to 2018-11-08, where the CB traded in-the-money and the rest of the period where the CB traded either at- or out-of-the-money. As seen in 4.14a the model delta performs well in the period where the CB trades in-the-money and poorly where the CB trades out-of-the-money. This makes it hard to find a modifying factor that fits the whole backtesting period. However, if we find a modifying factor for each of the periods the picture changes. When the CB trades in-the-money, the model delta proves to match the market delta and we do not need to use a modifying factor. In this period the hedged portfolio has a correlation with stock returns of -0.0842 and an average hedge error of -0.0001. Looking at where the CB trades at- or out-of-the-money the modifying factor is found to be 0.49, close to the modifying factor of 0.51 for TSLA.

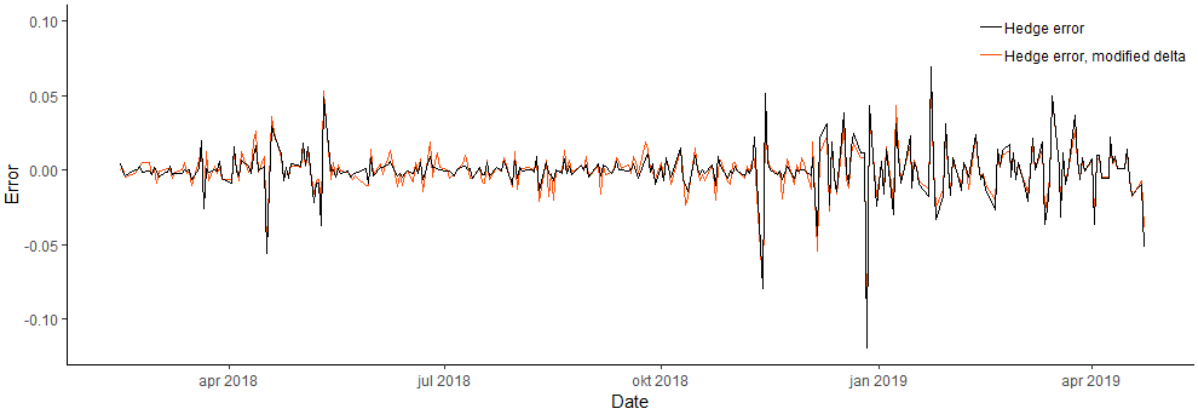

(a)

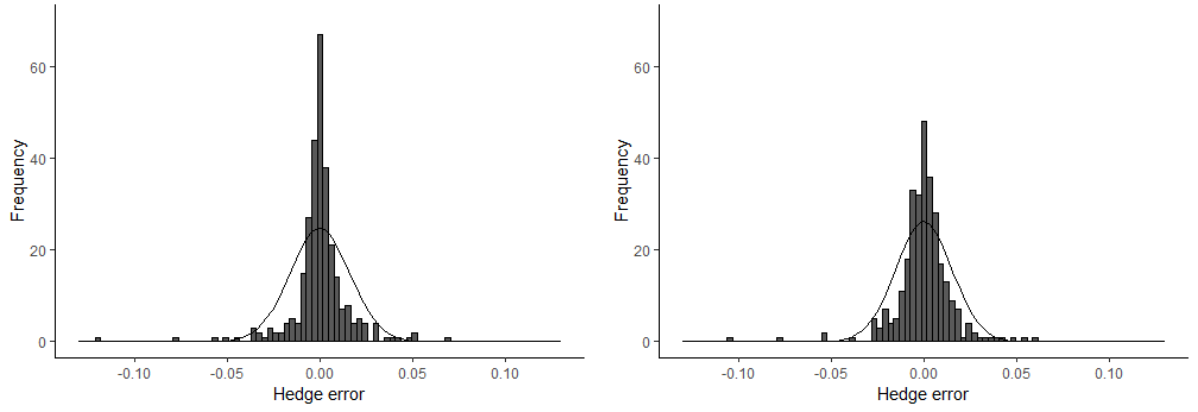

(b)

(c)

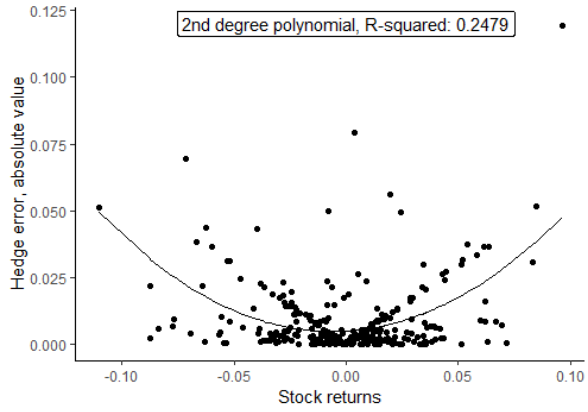

(d)

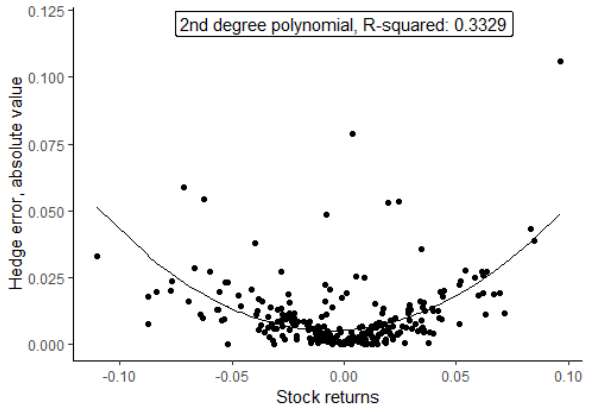

(e)

Figure 4.14: Hedging performance for RIG. (a) Hedging error over time. (b) Hedge error histogram, gaussian distribution n($\mu = -2.027e-4$, $\sigma = 0.0161$) superimposed. (c) Hedge error histogram, gaussian distribution n($\mu = -2.293e-4$, $\sigma = 0.0152$) superimposed. (d) Hedge error in absolute value on stock returns. (e) Hedge error in absolute value on stock returns.

Chapter 5

Discussion

The evidence from Section 4.3 clearly shows that the TSLA and RIG CBs are less sensitive to changes in the underlying stock price than the models suggest, i.e. the market delta is lower than the model delta. We suspect that the most likely factors affecting this deviation are:

- Illiquidity and transaction cost
- Moneyness
- Multiple day averages as input to valuation models
- Estimation error in model parameters

As CBs are less liquid and more costly to trade than the underlying stock, the price of the CB will be less sensitive to small stock price changes than if the CB had been perfectly liquid with zero transaction cost.

The second factor we suspect will affect the deviation between market and model deltas, f_ϵ, is moneyness. We define that the CB trades at-the-money if conversion would roughly give the same payoff as the face value of the bond, thus setting the strike price, K, where $S \cdot cr = F \implies K = \frac{F}{cr}$. A convertible bond that is at- or in-the-money will be more weighted towards its option component, and as shown in Figure E.2, the delta is more similar for different configurations of input parameters when the CB is more in-the-money. Also, as the delta here is high, the change in CB price as response to a price change in the underlying will be larger compared with transaction cost than for lower deltas associated with out-of-the-money bonds, which in turn should lessen the impact of transaction costs

on the sensitivity. For RIG this hypothesis is indeed supported by the data, as seen in Figure 5.1. In the period from 2018-04-11 to 2018-11-08 the RIG stock traded at prices such that the CB was in-the-money. In this period we observe from Figure 5.1b that the hedge error was significantly lower and more consistent than the rest of the period. The effect is really observable from 2018-05-14 to 2018-11-08, suggesting that it might take some time to adjust to the regime.

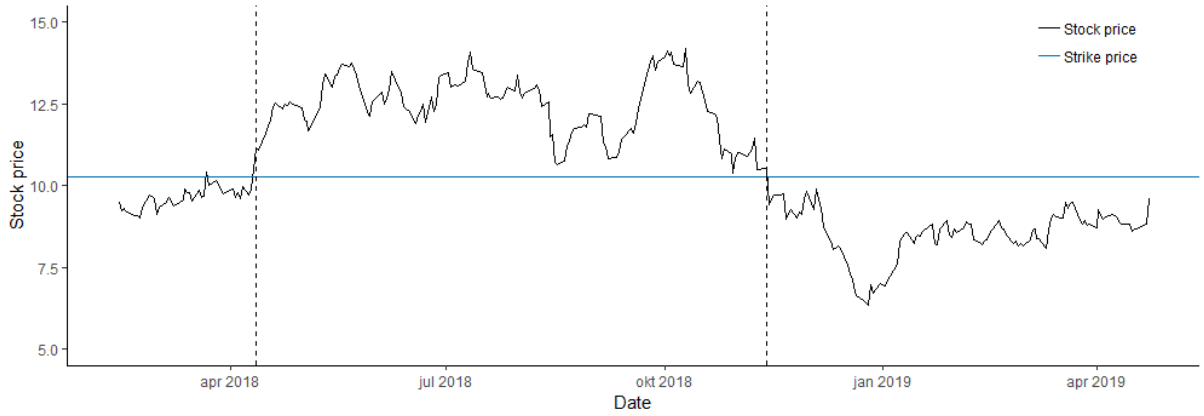

(a)

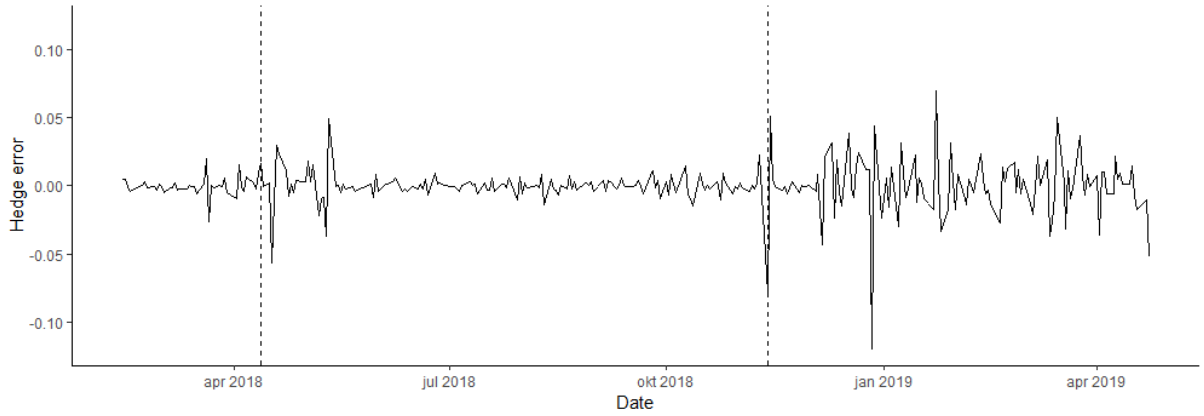

(b)

Figure 5.1: RIG: (a) Moneyness. (b) Hedge error. With the period 2018-04-11 to 2018-11-08 between the dashed lines.

Figure 5.2a shows that TSLA is mostly out-of-the-money in the period from 2018-02-01 to 2019-04-23, and only for short periods of time is the CB at- or slightly in-the-money. Hence the relationship found for RIG is not as evident for TSLA. As seen for RIG, there was a lag from when the stock started to trade above the strike price until the hedge error dampened. Thus, the fact that there are no prolonged in-the-money periods for TSLA may explain why we do not observe any correlation between moneyness and hedge error for TSLA in Figure 5.2.

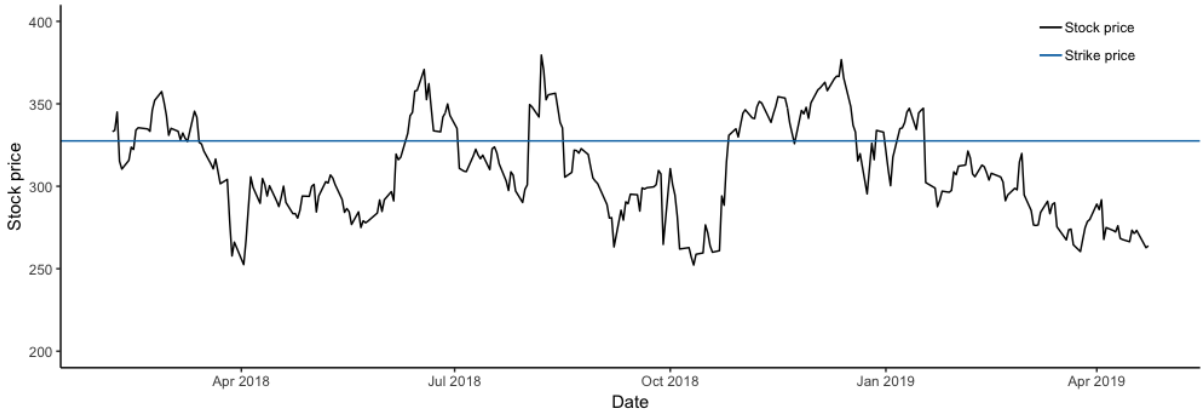

(a)

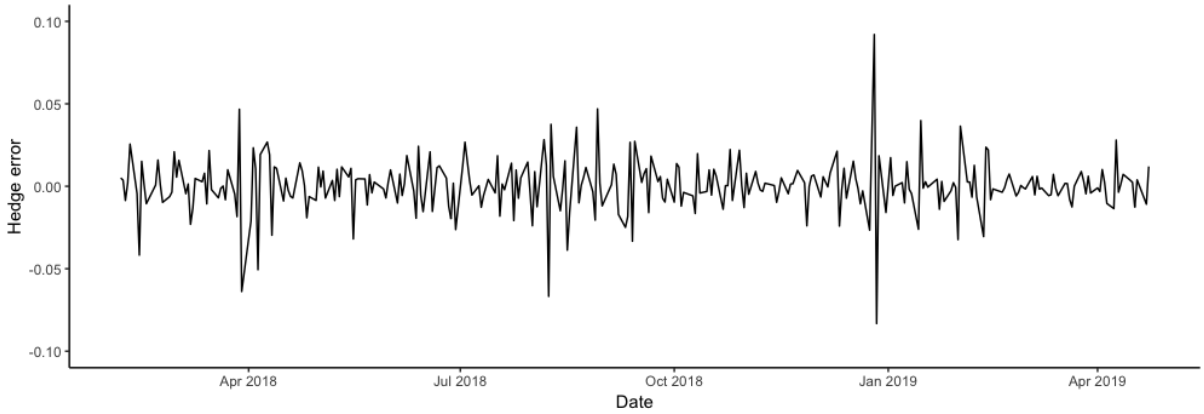

(b)

Figure 5.2: TSLA: (a) Moneyness. (b) Hedge error

When pricing CBs on a volatile stock as TSLA, it is likely that investors use a multiple day average stock price as input to their models. This would mean that while the model delta may be suitable to a multiple day average, it will be too high for daily stock prices. As mentioned, when running a regression of CB returns on stock returns we get a slope of 0.4248. Doing the same regression of the returns of 3-day average stock prices will however yield a slope of 0.6067, which is much closer to the average model delta of 0.6790, although at a reduction in R-squared from 0.3808 to 0.2688. As for RIG we do not find higher slopes on multiple day averages, so the hypothesis that market participants trade on multiple day averages, which in turn causes lower market deltas, does not hold in this case.

The last factor is estimation error of model parameters. Figure E.1 and E.2 in the Appendix show how the different model parameters affect both level and shape of the price curve. We see that the delta is most sensitive to p of Equation 2.6, recovery rate and equity volatility, all of which are unobservable and subject to great uncertainty.

As mentioned, p is the ratio between the credit spread volatility and equity volatility, both of which are unobservable and change frequently. The estimates of p that we obtained were unreasonably high, so we selected p to minimize pricing error. Also, this p was kept constant, which may not be a reasonable assumption.

The recovery rates were estimated from CDS spreads and the probability of default in the DataGrapple database, but we suspect that the probability of default is computed from the CDS spreads using an assumed recovery rate rather than from a traded instrument. Hence, the recovery rate we use is the average recovery rate of all outstanding bonds from the issuing company, assumed by Hellebore Capital. This may deviate from recovery rates of the CBs assumed by other market participants. Also, the assumption of constant recovery rates over the time period we analyze may be unreasonable. As noted earlier, the effect of R on delta diminishes as the CB increases in moneyness.

The equity volatility is estimated using a GARCH(1,1) model over a substantially longer time period than the one selected for analysis in this thesis and could deviate from the volatility assumed by investors at each point in time. Investors will use a combination of historical returns and future expectations in their volatility assumptions and unless their future expectations actually materialized their estimates will deviate from the GARCH estimate. We have also not accounted for any potential structural shifts in volatility which would require different GARCH models for different time periods.

Lastly, due to the lack of historical option prices, we assume constant term structures for the volatility and credit spread over the whole period. As the outlook for the future tends to vary, this assumption affects our results and is a factor of uncertainty. We try to adjust for this by parallel shifting the volatility term structure, but the shape of the structure is still the same. Assuming that the market expects the long-term volatility to remain the same, the implied volatility of the options close to maturity will rise more than the ones with maturity further away when the volatility increases, resulting in an altered shape of the curve. When simply parallel shifting the term structure we might introduce an overestimation of the long-term volatility used in the model in times with high volatility, leading to an overestimation of the price and delta. This effect can be observed for RIG around 2019-01, by looking at the volatility in Figure 4.7 and the price error in Figure 4.10.

Chapter 6

Conclusion

This thesis adds to the existing literature by empirically testing the applicability of the AFV model in convertible arbitrage strategies, with particular focus on delta hedging. We find that while the model is able to compute prices in accordance with market prices, the delta is generally too high. More specifically, the model delta is about twice the market delta for both TSLA and RIG, when the CB is at- or out-the-money. We also show that by applying a suitable tuning factor f_ϵ we are able to obtain good delta estimates that virtually eliminate equity risk from small stock returns. We further demonstrate that between a quarter (TSLA) and a third (RIG) of the residual hedging risk can be explained by the convexity of the CB, gamma, a known issue from the theory of delta hedging.

We propose that illiquidity and transaction costs, moneyness, the use of multiple day averages in valuation models and estimation error in model parameters are the main sources of the difference between the model delta and the market delta. However, our bond sample is not sufficiently large to draw any general conclusions in this regard.

Further research should use a larger bond sample for analysis, which would average out company specific effects to better analyze the delta hedging capabilities of the AFV model. The model could quite easily be extended to incorporate put and call provisions, which would widen the scope of potential convertible bonds for analysis. We were also limited to publicly available data sources which affects both the sample size and the accuracy of

the price and delta estimates. Access to more CDS data would significantly increase the size of the sample. Also, the lack of historical call option prices made us assume constant shape of the term structure of volatility, which may be an unreasonable assumption.

Accompanied by a larger bond sample future research should investigate how different factors affect the discrepancy between the deltas from the model and those of the market. With extensive historical trading data one can easily estimate the appropriate delta with regressions or minimization of squared correlations, but for newly listed bonds it will be difficult to determine the appropriate reducing factor without any general predictive models.

Bibliography

Ammann, M., Kind, A., and Wilde, C. (2008). Simulation-based pricing of convertible bonds. *Journal of empirical finance*, 15(2):310–331.

Ammann, M. and Seiz, R. (2006). Pricing and hedging mandatory convertible bonds. *Journal of Derivatives*, 13(3):30–46.

Andersen, L. B. and Buffum, D. (2002). Calibration and implementation of convertible bond models. *Available at SSRN 355308*.

Ayache, E., Forsyth, P. A., and Vetzal, K. R. (2003). The valuation of convertible bonds with credit risk. Technical report, Cornell University.

Black, F. and Cox, J. C. (1976). Valuing corporate securities: Some effects of bond indenture provisions. *The Journal of Finance*, 31(2):351–367.

Black, F. and Scholes, M. (1973). The pricing of options and corporate liabilities. *Journal of political economy*, 81(3):637–654.

Brennan, M. J. and Schwartz, E. S. (1977). Convertible bonds: Valuation and optimal strategies for call and conversion. *The Journal of Finance*, 32(5):1699–1715.

Brennan, M. J. and Schwartz, E. S. (1980). Analyzing convertible bonds. *The Journal of Financial and Quantitative Analysis*, 15(4):907–929.

David Frank, B. (2018). Ovcv model description. *Quantitative Finance and Development, Equities Team, May 15, 2014*.

Dixit & Pindyck, Avinash K., R. S. (1994). *Investment under Uncertainty*. Princeton University Press.

Gabelli (2018). A review of the convertible securities market, gabelli funds. `https://www.gabelli.com/Gab_pdf/Insights/Convertible_White_Paper.pdf`. Accessed: 2018-11-13.

GoldmanSachs (1994). Valuing convertible bonds as derivatives. *Quantitative strategies research notes*, 11(1):30.

Ingersoll Jr, J. E. (1977). A contingent-claims valuation of convertible securities. *Journal of Financial Economics*, 4(3):289–321.

Kreyszig, E. (2010). *Advanced Engineering Mathematics*. John Wiley & Sons.

Loncarski, I., Ter Horst, J., and Veld, C. (2009). The rise and demise of the convertible arbitrage strategy. *Financial Analysts Journal*, 65(5):35–50.

Merton, R. C. (1974). On the pricing of corporate debt: The risk structure of interest rates. *The Journal of finance*, 29(2):449–470.

Muromachi, Y. (1999). The growing recognition of credit risk in corporate and financial bond markets. *NLI Research Institute, Paper*, 126.

Tsiveriotis, K. and Fernandes, C. (1998). Valuing convertible bonds with credit risk. *Journal of Fixed Income*, 8(2):95–102.

Zabolotnyuk, Y., Jones, R., and Veld, C. (2010). An empirical comparison of convertible bond valuation models. *Financial Management*, 39(2):675–706.

Appendix A

Derivation of SDE

$$dx = a(x,t)dt + b(x,t)dz + g(x,t)dq,\ dz \sim N(0,1),\ dq = \begin{cases} 1, & \text{p= } \lambda dt \\ 0 & \text{p= } (1-\lambda dt) \end{cases} \tag{A.1}$$

For a stochastic jump-diffusion process as described in Equation A.1, a special version of Ito's Lemma is used for the valuation of a contingent claim, $H(x,t)$. The expected value of this Ito expansion is as given in Equation A.2 (Dixit & Pindyck, 1994).

$$E[dH] = \left[\frac{\partial H}{\partial t} + a(x,t)\frac{\partial H}{\partial x} + \frac{1}{2}b(x,t)^2\frac{\partial^2 H}{\partial x^2}\right]dt + \lambda dt\left[H(x+g(x,t),t) - H(x,t)\right] \tag{A.2}$$

In this case $x = S$, and $a(S,t) = (r + \lambda\eta - \delta)S$, $b(S,t) = \sigma S$ and $g(S,t) = -\eta S$.

Let the bond component be denoted $B(S,t)$. In the case of default we have that $B(S(1-\eta),t) = RX$ and using Equation A.2 we obtain:

$$E[dB] = \left[\frac{\partial B}{\partial t} + (r + \lambda\eta - \delta)S\frac{\partial B}{\partial S} + \frac{1}{2}\sigma^2 S^2\frac{\partial^2 B}{\partial S^2}\right]dt + \lambda dt\left[RX - B(S,t)\right] \tag{A.3}$$

Given that default risk is diversifiable we have that $rBdt = E[dB]$, and Equation A.4 becomes:

$$rBdt = \left[\frac{\partial B}{\partial t} + (r + \lambda\eta - \delta)S\frac{\partial B}{\partial S} + \frac{1}{2}\sigma^2 S^2\frac{\partial^2 B}{\partial S^2}\right]dt + \lambda dtRX - \lambda dtB \tag{A.4}$$

Dividing by dt, letting $X = F$ and rewriting using subscript to denote partial derivatives we obtain the following:

$$B_t = -(\frac{\sigma^2}{2}S^2 B_{SS} + (r + \lambda\eta - \delta)SB_S - (r + \lambda)B) - \lambda RF \tag{A.5}$$

Defining $\tau = T - t$, the equation changes to:

$$B_\tau = (\frac{\sigma^2}{2}S^2 B_{SS} + (r + \lambda\eta - \delta)SB_S - (r + \lambda)B) + \lambda RF \tag{A.6}$$

The derivation for the option component C is the same except that
$\lambda dt\,[H(x + g(x,t), t) - H(x,t)]$, the expected change in the case of a jump from Equation A.2, becomes $\lambda dt \cdot max[\kappa \cdot S(1 - \eta) - RF, 0]$. Hence we get the following:

$$C_t = -(\frac{\sigma^2}{2}S^2 C_{SS} + (r + \lambda\eta - \delta)SC_S - (r + \lambda)C) - \lambda \max[\kappa S(1 - \eta) - RF, 0] \tag{A.7}$$

Defining $\tau = T - t$, the equation changes to:

$$C_\tau = (\frac{\sigma^2}{2}S^2 C_{SS} + (r + \lambda\eta - \delta)SC_S - (r + \lambda)C) + \lambda \max[\kappa S(1 - \eta) - RF, 0] \tag{A.8}$$

This system is solved looping backwards from maturity with the following boundary conditions:

At maturity:

$$B_T = (F + F \cdot \frac{cpn}{2}) \left(1 - \frac{\lambda_T}{1 + \lambda_T}\right) + RF\frac{\lambda_T}{1 + \lambda_T} \tag{A.9}$$

$$C_T = \begin{cases} \kappa S - B_T & B_T < \kappa S \\ 0 & \text{otherwise} \end{cases} \tag{A.10}$$

At stock price equal to zero, i.e. default, we use Equation A.8 and Equation A.6 with $S = 0$ inserted as BC.

Appendix B

Derivation of the Crank-Nicolson scheme

As mentioned, the Crank-Nicolson scheme is the average of the forward and backward Euler method. In the derivation of the Crank-Nicolson scheme we use θ as the degree of forward Euler. By setting $\theta = \frac{1}{2}$ one obtains the Crank- Nicolson method we use to solve the equations derived in App. A. Note that i denotes stockprice i, while k denotes timestep $\tau = T - t$ on the time-stockprice grid. First we introduce:

Time derivative:

$$\frac{\partial C}{\partial \tau} = \frac{C_i^{k+1} - C_i^k}{\Delta \tau} \tag{B.1}$$

Delta:

$$\frac{\partial C}{\partial S} = \theta \frac{C_{i+1}^{k+1} - C_{i-1}^{k+1}}{2\Delta S} + (1-\theta)\frac{C_{i+1}^{k} - C_{i-1}^{k}}{2\Delta S} \tag{B.2}$$

Gamma:

$$\frac{\partial^2 C}{\partial S^2} = \theta \frac{C_{i+1}^{k+1} - 2C_i^{k+1} + C_{i-1}^{k+1}}{(\Delta S)^2} + (1-\theta)\frac{C_{i+1}^{k} - 2C_i^{k} + C_{i-1}^{k}}{(\Delta S)^2} \tag{B.3}$$

Discretizing Equation A.6 on the time-stock price grid we get:

$$\begin{aligned} \frac{B_i^{k+1} - B_i^k}{\Delta \tau} = \frac{\sigma^2}{2} S_i^2 \left[\theta \frac{B_{i+1}^{k+1} - 2B_i^{k+1} + B_{i-1}^{k+1}}{(\Delta S)^2} + (1-\theta)\frac{B_{i+1}^{k} - 2B_i^{k} + B_{i-1}^{k}}{(\Delta S)^2} \right] \\ + (r + \lambda\eta - \Delta) S_i \left[\theta \frac{B_{i+1}^{k+1} - B_{i-1}^{k+1}}{2\Delta S} + (1-\theta)\frac{B_{i+1}^{k} - B_{i-1}^{k}}{2\Delta S} \right] \\ - \theta[(r+\lambda)B_i^{k+1} - \lambda RF] - (1-\theta)[(r+\lambda)B_i^k - \lambda RF] \end{aligned} \tag{B.4}$$

We rearrange:

$$\begin{aligned}&\frac{B_i^{k+1}-B_i^k}{\Delta\tau}=\\&\theta\left[\frac{\sigma^2}{2}S_i^2\frac{B_{i+1}^{k+1}-2B_i^{k+1}+B_{i-1}^{k+1}}{(\Delta S)^2}+(r+\lambda\eta-\Delta)S_i\frac{B_{i+1}^{k+1}-B_{i-1}^{k+1}}{2\Delta S}-(r+\lambda)B_i^{k+1}+\lambda RF\right]\\&+(1-\theta)\left[\frac{\sigma^2}{2}S_i^2\frac{B_{i+1}^{k}-2B_i^{k}+B_{i-1}^{k}}{(\Delta S)^2}+(r+\lambda\eta-\Delta)S_i\frac{B_{i+1}^{k}-B_{i-1}^{k}}{2\Delta S}-(r+\lambda)B_i^{k}+\lambda RF\right]\end{aligned} \tag{B.5}$$

As for C we discretize Equation A.8, where we assume that we recover a fraction of the face value of the bond, i.e $X = F$ and get:

$$\begin{aligned}\frac{C_i^{k+1}-C_i^k}{\Delta\tau}=\theta\Bigg[&\frac{\sigma^2}{2}S^2\frac{C_{i+1}^{k+1}-2C_i^{k+1}+C_{i-1}^{k+1}}{(\Delta S)^2}+(r+\lambda\eta-\Delta)S_i\frac{C_{i+1}^{k+1}-C_{i-1}^{k+1}}{2\Delta S}\\&-(r+\lambda)C_i^{k+1}+\lambda\max(\kappa S_i(1-\eta)-RF,0)\Bigg]\\+(1-\theta)\Bigg[&\frac{\sigma^2}{2}S_i^2\frac{C_{i+1}^{k}-2C_i^{k}+C_{i-1}^{k}}{(\Delta S)^2}+(r+\lambda\eta-\Delta)S_i\frac{C_{i+1}^{k}-C_{i-1}^{k}}{2\Delta S}\\&-(r+\lambda)C_i^{k}+\lambda\max(\kappa S_i(1-\eta)-RF,0)\Bigg]\end{aligned} \tag{B.6}$$

By varying θ we get different methods. Some common methods are:

$$\begin{aligned}\theta=1&\quad\text{Forward Euler Method}\\\theta=0&\quad\text{Backward Euler Method}\\\theta=\tfrac{1}{2}&\quad\text{Crank-Nicolson Method}\end{aligned}$$

Setting $\theta = \frac{1}{2}$ we obtain the Crank-Nicolson method:

$$\begin{aligned}&\frac{B_i^{k+1}-B_i^k}{\Delta\tau}=\\&\left[\frac{\sigma^2}{4}S_i^2\frac{B_{i+1}^{k+1}-2B_i^{k+1}+B_{i-1}^{k+1}}{(\Delta S)^2}+(r+\lambda\eta-\Delta)S_i\frac{B_{i+1}^{k+1}-B_{i-1}^{k+1}}{4\Delta S}-\frac{1}{2}(r+\lambda)B_i^{k+1}\right]\\&+\left[\frac{\sigma^2}{4}S_i^2\frac{B_{i+1}^{k}-2B_i^{k}+B_{i-1}^{k}}{(\Delta S)^2}+(r+\lambda\eta-\Delta)S_i\frac{B_{i+1}^{k}-B_{i-1}^{k}}{4\Delta S}-\frac{1}{2}(r+\lambda)B_i^{k}\right]+\lambda RF\end{aligned} \tag{B.7}$$

$$\begin{aligned}\frac{C_i^{k+1}-C_i^k}{\Delta\tau} = \\ \left[\frac{\sigma^2}{4}S_i^2\,\frac{C_{i+1}^{k+1}-2C_i^{k+1}+C_{i-1}^{k+1}}{(\Delta S)^2}+(r+\lambda\eta-\Delta)S_i\frac{C_{i+1}^{k+1}-C_{i-1}^{k+1}}{4\Delta S}-\frac{1}{2}(r+\lambda)C_i^{k+1}\right] \\ +\left[\frac{\sigma^2}{4}S_i^2\frac{C_{i+1}^{k}-2C_i^{k}+C_{i-1}^{k}}{(\Delta S)^2}+(r+\lambda\eta-\Delta)S_i\frac{C_{i+1}^{k}-C_{i-1}^{k}}{4\Delta S}-\frac{1}{2}(r+\lambda)C_i^{k}\right] \\ +\lambda\max[\kappa S_i(1-\eta)-RF,0]\end{aligned} \tag{B.8}$$

Rearranging, we obtain some common coefficients:

$$\begin{aligned}B_i^{k+1}\left[1+\frac{\sigma^2S_i^2\Delta\tau}{2(\Delta S)^2}+\frac{\Delta\tau}{2}(r+\lambda)\right]=B_{i+1}^{k+1}\left[\frac{\sigma^2S_i^2\Delta\tau}{4(\Delta S)^2}+\frac{(r+\lambda\eta-\Delta)S_i\Delta\tau}{4\Delta S}\right] \\ +B_{i+1}^{k}\left[\frac{\sigma^2S_i^2\Delta\tau}{4(\Delta S)^2}+\frac{(r+\lambda\eta-\Delta)S_i\Delta\tau}{4\Delta S}\right]+B_{i-1}^{k+1}\left[\frac{\sigma^2S_i^2\Delta\tau}{4(\Delta S)^2}-\frac{(r+\lambda\eta-\Delta)S_i\Delta\tau}{4\Delta S}\right] \\ +B_{i-1}^{k}\left[\frac{\sigma^2S_i^2\Delta\tau}{4(\Delta S)^2}-\frac{(r+\lambda\eta-\Delta)S_i\Delta\tau}{4\Delta S}\right]+B_i^{k}\left[1-\frac{\sigma^2S_i^2\Delta\tau}{2(\Delta S)^2}-\frac{\Delta\tau}{2}(r+\lambda)\right]+\Delta\tau\lambda RF\end{aligned} \tag{B.9}$$

$$\begin{aligned}C_i^{k+1}\left[\frac{1}{\Delta\tau}+\frac{\sigma^2S_i^2}{2(\Delta S)^2}+\frac{1}{2}(r+\lambda)\right]=C_{i+1}^{k+1}\left[\frac{\sigma^2S_i^2}{4(\Delta S)^2}+\frac{(r+\lambda\eta-\Delta)S_i}{4}\right] \\ +C_{i-1}^{k+1}\left[\frac{\sigma^2S_i^2}{4(\Delta S)^2}-\frac{(r+\lambda\eta-\Delta)S_i}{4}\right]+C_{i+1}^{k}\left[\frac{\sigma^2S_i^2}{4(\Delta S)^2}+\frac{(r+\lambda\eta-\Delta)S_i}{4}\right] \\ +C_i^{k}\left[\frac{1}{\Delta\tau}-\frac{\sigma^2S_i^2}{2(\Delta S)^2}-\frac{1}{2}(r+\lambda)\right]+C_{i-1}^{k}\left[\frac{\sigma^2S^2}{4(\Delta S)^2}-\frac{(r+\lambda\eta-\Delta)S_i}{4}\right] \\ +\lambda\max[\kappa S_i(1-\eta)-RF,0]\end{aligned} \tag{B.10}$$

Solving for B_i^{k+1} and C_i^{k+1} we obtain the following expressions:

$$B_i^{k+1}=\frac{\alpha_i(B_{i+1}^{k+1}+B_{i+1}^{k})+\beta_i(B_{i-1}^{k+1}+B_{i-1}^{k})+B_i^k(2-(\alpha_i+\beta_i)-(r+\lambda)\Delta\tau)+2\Delta\tau\lambda RF}{2+\alpha_i+\beta_i+(r+\lambda)\Delta\tau} \tag{B.11}$$

$$C_i^{k+1}=\frac{\alpha_i(C_{i+1}^{k+1}+C_{i+1}^{k})+\beta_i(C_{i-1}^{k+1}+C_{i-1}^{k})+C_i^k(2-(\alpha_i+\beta_i)-(r+\lambda)\Delta\tau)+2\lambda\Delta\tau\max[\kappa S_i(1-\eta)-RF,0]}{2+\alpha_i+\beta_i+(r+\lambda)\Delta\tau} \tag{B.12}$$

Where: $\alpha_i=\frac{\sigma^2S_i^2\Delta t}{2\Delta S^2}+\frac{S_i(r+\lambda\eta-\Delta)\Delta t}{2\Delta S}$ and $\beta_i=\frac{\sigma^2S_i^2\Delta t}{2\Delta S^2}-\frac{S_i(r+\lambda\eta-\Delta)\Delta t}{2\Delta S}$

Appendix C

Fokker-Planck equation

The Fokker-Planck equation for a convection-diffusion process, such as Merton's jump-diffusion process, describes the time-evolution of the probability density of the stock price. As in Andersen and Buffum (2002), we use the equation for the log-stock price space instead of the regular stock price space, and discount the probabilities with the rates on the RHS of the equation. The equation becomes the following:

$$-\frac{\partial p}{\partial s}-\frac{\partial}{\partial y}(r-q+\lambda-\frac{1}{2}\sigma^2)p+\frac{1}{2}\frac{\partial^2}{\partial y^2}\sigma^2 p=(r+\lambda)p \tag{C.1}$$

This can be rewritten as:

$$-\frac{\partial p}{\partial s}-H(s,y)\frac{\partial p}{\partial y}+\frac{1}{2}\sigma(s,e^y)^2\frac{\partial^2 p}{\partial y^2}=G(s,y)p \tag{C.2}$$

where:

$$H(s,y)=r(s)-q(s)+\lambda(s,e^y)-\frac{1}{2}\sigma(s,e^y)^2-2e^y\sigma(s,e^y)\frac{\partial\sigma}{\partial S} \tag{C.3}$$

$$G(s,y)=r(s)+\lambda(s,e^y)+e^y\lambda'(s,e^y)-e^y(\sigma(s,e^y)\left[2\sigma'(s,e^y)+e^y\sigma''(s,e^y)\right]+e^y\sigma'(s,e^y)^2) \tag{C.4}$$

where λ', σ' and σ'' is the partial derivatives with respect to S. By setting $\sigma(t,S)=b(t)$ and $\lambda(t,S)=a(t)(\frac{S(0)}{S})^p$, the terms $\frac{\partial\sigma}{\partial S}$ and $\frac{\partial^2\sigma}{\partial S^2}$ vanish:

$$H(s,y) = r - q + a(s)(\frac{e^z}{e^y})^p - \frac{1}{2}b(s)^2 \tag{C.5}$$

$$G(s,y) = r + a(s)(\frac{e^z}{e^y})^p - pa(s)e^{pz}(\frac{1}{e^{y(p+1)}}) \tag{C.6}$$

We then discretize the equations and use subscripts, where i denotes the timestep, y is the natural logarithm of the stock price and z is the natural logarithm of the current stock price:

$$G_y^i = r + a^i(\frac{e^z}{e^y})^p - pa^i e^{pz}\frac{1}{e^{y(p+1)}} \tag{C.7}$$

$$H_y^i = r - q + a^i(\frac{e^z}{e^y})^p - \frac{1}{2}(b^i)^2 \tag{C.8}$$

By setting

$$D = -H\delta_y + \frac{1}{2}\sigma^2\delta_{yy} - G \tag{C.9}$$

where δ_y and δ_{yy} are the first and second difference operators with regard to y, $\delta_y p_y^i = \frac{p_{y+1}^i - p_{y-1}^i}{2\Delta y}$ and $\delta_{yy}p_y^i = \frac{p_{y+1}^i - 2p_y^i + p_{y-1}^i}{(\Delta y)^2}$.

we can further simplify the Equation C.2 to:

$$(\Delta T_i^{-1} - \theta D)p(T_{i+1}, y) = (\Delta T_i^{-1} + (1-\theta)D)p(T_i, y) \tag{C.10}$$

$$\frac{p_y^{i+1} - p_y^i}{\Delta T} = \theta D p_y^{i+1} + (1-\theta)Dp_y^i \tag{C.11}$$

$$\frac{p_y^{i+1} - p_y^i}{\Delta T} = \theta\left[-H_y^{i+1}\delta_y + \frac{1}{2}\sigma^2\delta_{yy} - G_y^{i+1}\right]p_y^{i+1} + (1-\theta)\left[-H_y^i\delta_y + \frac{1}{2}\sigma^2\delta_{yy} - G_y^i\right]p_y^i \tag{C.12}$$

Setting $\theta = \frac{1}{2}$ and inserting for the first and second difference operators, eq. C.12 will discretize to:

$$\begin{aligned}\frac{p_y^{i+1} - p_y^i}{\Delta T} = \frac{1}{2}\Bigg[&-H_y^{i+1}\frac{p_{y+1}^{i+1} - p_{y-1}^{i+1}}{2\Delta y} + \frac{1}{2}\sigma^2\frac{p_{y+1}^{i+1} - 2p_y^{i+1} + p_{y-1}^{i+1}}{(\Delta y)^2} - G_y^{i+1}p_y^{i+1}\Bigg] \\ &+\frac{1}{2}\Bigg[-H_y^i\frac{p_{y+1}^i - p_{y-1}^i}{2\Delta y} + \frac{1}{2}\sigma^2\frac{p_{y+1}^i - 2p_y^i + p_{y-1}^i}{(\Delta y)^2} - G_y^i p_y^i\Bigg]\end{aligned} \tag{C.13}$$

Furthermore, solving for p_y^{i+1} yields:

$$\begin{aligned} p_y^{i+1}\left[1+\frac{\sigma^2\Delta T}{2(\Delta y)^2}+\frac{G_y^{i+1}\Delta T}{2}\right] &= p_{y+1}^{i+1}\left[\frac{-H_y^{i+1}\Delta T}{4\Delta y}+\frac{\sigma^2\Delta T}{4(\Delta y)^2}\right] \\ &+p_{y+1}^{i}\left[\frac{-H_y^{i}\Delta T}{4\Delta y}+\frac{\sigma^2\Delta T}{4(\Delta y)^2}\right]+p_{y-1}^{i+1}\left[\frac{H_y^{i+1}\Delta T}{4\Delta y}+\frac{\sigma^2\Delta T}{4(\Delta y)^2}\right] \\ &+p_{y-1}^{i}\left[\frac{H_y^{i}\Delta T}{4\Delta y}+\frac{\sigma^2\Delta T}{4(\Delta y)^2}\right]+p_{y}^{i}\left[1-\frac{\sigma^2\Delta T}{2(\Delta y)^2}-\frac{G_y^{i}\Delta T}{2}\right] \end{aligned} \tag{C.14}$$

$$p_y^{i+1}=\frac{p_{y+1}^{i+1}\alpha_y^{i+1}+p_{y+1}^{i}\alpha_y^{i}+p_{y-1}^{i+1}\beta_y^{i+1}+p_{y-1}^{i}\beta_y^{i}+p_y^i[2-(\alpha_y^i+\beta_y^i)-G_y^i\Delta T]}{2+\alpha_y^{i+1}+\beta_y^{i+1}+G_y^{i+1}\Delta T} \tag{C.15}$$

Where $\alpha_y^i=\frac{-H_y^i\Delta T}{2\Delta y}+\frac{\sigma^2\Delta T}{2(\Delta y)^2}$ and $\beta_y^i=\frac{H_y^i\Delta T}{2\Delta y}+\frac{\sigma^2\Delta T}{2(\Delta y)^2}$.

Appendix D

Upwind Discretization

To deal with the loss of probability experienced using the regular discretization scheme we instead implement upwind discretization to the Fokker-Planck equation:

$$-\frac{\partial p}{\partial s}-\frac{\partial}{\partial y}(r-q+\lambda-\frac{1}{2}\sigma^2)p+\frac{1}{2}\frac{\partial^2}{\partial y^2}\sigma^2 p=(r+\lambda)p \tag{D.1}$$

First we set $\sigma(s,e^y)=\sigma(s)$. By using the upwind discretization scheme we approximate $\frac{\partial}{\partial y}(r-q+\lambda-\frac{1}{2}\sigma^2)p \sim D_h((r-q+\lambda-\frac{1}{2}\sigma^2)p)$, where D_h is the difference approximation. Then the Fokker-Plank equation can be discretized as:

$$\begin{aligned}-\frac{p_y^{i+1}-p_y^i}{\Delta s}=(1-\theta)\Bigg[&\frac{(r-q+\lambda_{y+1}^i-\frac{1}{2}\sigma^2)p_{y+1}^i-(r-q+\lambda_{y-1}^i-\frac{1}{2}\sigma^2)p_{y-1}^i}{2\Delta y}\\&-\frac{1}{2}\sigma^2(\frac{p_{y+1}^i-2p_y^i+p_{y-1}^i}{\Delta y^2})+(r+\lambda_y^i)p_y^i\Bigg]\\+\theta\Bigg[&\frac{(r-q+\lambda_{y+1}^{i+1}-\frac{1}{2}\sigma^2)p_{y+1}^{i+1}-(r-q+\lambda_{y-1}^{i+1}-\frac{1}{2}\sigma^2)p_{y-1}^{i+1}}{2\Delta y}\\&-\frac{1}{2}\sigma^2(\frac{p_{y+1}^{i+1}-2p_y^{i+1}+p_{y-1}^{i+1}}{\Delta y^2})+(r+\lambda_y^{i+1})p_y^{i+1}\Bigg]\end{aligned} \tag{D.2}$$

We then set $c=r-q-\frac{1}{2}\sigma^2$ and get:

$$\begin{aligned}&\frac{p_y^{i+1}-p_y^i}{\Delta s}=\\&-(1-\theta)\left[\frac{(c+\lambda_{y+1}^i)p_{y+1}^i-(c+\lambda_{y-1}^i)p_{y-1}^i}{2\Delta y}-\frac{1}{2}\sigma^2(\frac{p_{y+1}^i-2p_y^i+p_{y-1}^i}{\Delta y^2})+(r+\lambda_y^i)p_y^i\right]\\&-\theta\left[\frac{(c+\lambda_{y+1}^{i+1})p_{y+1}^{i+1}-(c+\lambda_{y-1}^{i+1})p_{y-1}^{i+1}}{2\Delta y}-\frac{1}{2}\sigma^2(\frac{p_{y+1}^{i+1}-2p_y^{i+1}+p_{y-1}^{i+1}}{\Delta y^2})+(r+\lambda_y^{i+1})p_y^{i+1}\right]\end{aligned} \tag{D.3}$$

$$
\begin{aligned}
p_y^{i+1}\left[1+\theta\left(\frac{\sigma^2\Delta s}{(\Delta y)^2}+(r+\lambda_y^{i+1})\Delta s\right)\right] &= p_{y+1}^{i+1}\left[-\theta\left(\frac{(c+\lambda_{y+1}^{i+1})\Delta s}{2\Delta y}-\frac{\sigma^2\Delta s}{2\Delta y^2}\right)\right] \\
+p_{y+1}^{i}\left[-(1-\theta)\left(\frac{(c+\lambda_{y+1}^{i})\Delta s}{2\Delta y}-\frac{\sigma^2\Delta s}{2\Delta y^2}\right)\right] &+ p_{y-1}^{i+1}\left[\theta\left(\frac{(c+\lambda_{y-1}^{i+1})\Delta s}{2\Delta y}+\frac{\sigma^2\Delta s}{2\Delta y^2}\right)\right] \\
+p_{y-1}^{i}\left[(1-\theta)\left(\frac{(c+\lambda_{y-1}^{i})\Delta s}{2\Delta y}+\frac{\sigma^2\Delta s}{2\Delta y^2}\right)\right] &+ p_y^i\left[1-(1-\theta)\left(\frac{\sigma^2\Delta s}{(\Delta y)^2}+(r+\lambda_y^i)\Delta s\right)\right]
\end{aligned}
\tag{D.4}
$$

$$
p_y^{i+1}=\frac{p_{y+1}^{i+1}\alpha_{y+1}^{i+1}+p_{y+1}^{i}\alpha_{y+1}^{i}+p_{y-1}^{i+1}\beta_{y-1}^{i+1}+p_{y-1}^{i}\beta_{y-1}^{i}+p_y^i\left[2-\frac{\sigma^2\Delta s}{(\Delta y)^2}-(r+\lambda_y^i)\Delta s\right]}{2+\frac{\sigma^2\Delta s}{(\Delta y)^2}+(r+\lambda_y^{i+1})\Delta s} \tag{D.5}
$$

Where $\alpha_{y+1}^{i+1}=\frac{\sigma^2\Delta s}{2\Delta y^2}-\frac{(c+\lambda_{y+1}^{i+1})\Delta s}{2\Delta y}$, $\beta_{y-1}^{i+1}=\frac{\sigma^2\Delta s}{2\Delta y^2}+\frac{(c+\lambda_{y-1}^{i+1})\Delta s}{2\Delta y}$, $\alpha_{y+1}^{i}=\frac{\sigma^2\Delta s}{2\Delta y^2}-\frac{(c+\lambda_{y+1}^{i})\Delta s}{2\Delta y}$, $\beta_{y-1}^{i}=\frac{\sigma^2\Delta s}{2\Delta y^2}+\frac{(c+\lambda_{y-1}^{i})\Delta s}{2\Delta y}$

Note that this discretization has two different α and β values that captures more closely the changes in $\lambda=a(t)(\frac{e^z}{e^y})^p$, which changes rapidly with y, especially for high values of p.

Appendix E

Sensitivity plots

In this chapter we present the price and delta sensitivity of the AFV model to the different input parameters, p, R, volatility, credit spread, η and risk free rate. We see that the parameter with the biggest impact on price and delta is the recovery rate, R. We also observe that all but one parameter, volatility, mostly affect the distressed and out-of-the-money area. This is because all the parameters except volatility have influence on the bond component, whereas volatility affects the equity component.

We also show the sensitivity of a(t) and b(t) to p, as presented by Andersen and Buffum (2002). Note that the time horizon in Figure E.3 is significantly longer than the ones evaluated in this thesis, with 15 years compared to 5 years. Also bear in mind that Figure E.3 is created using constant implied volatility and credit spread structure, unlike the calibration in our model.

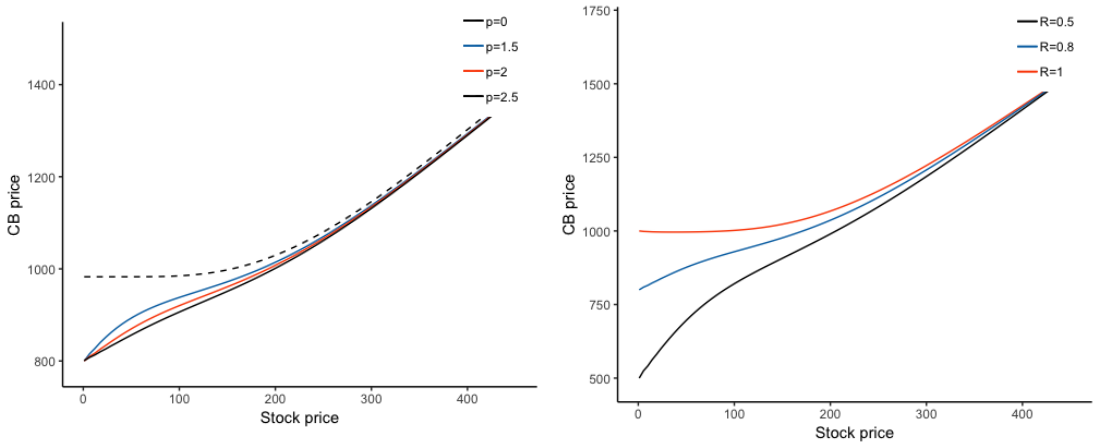

(a) p

(b) R

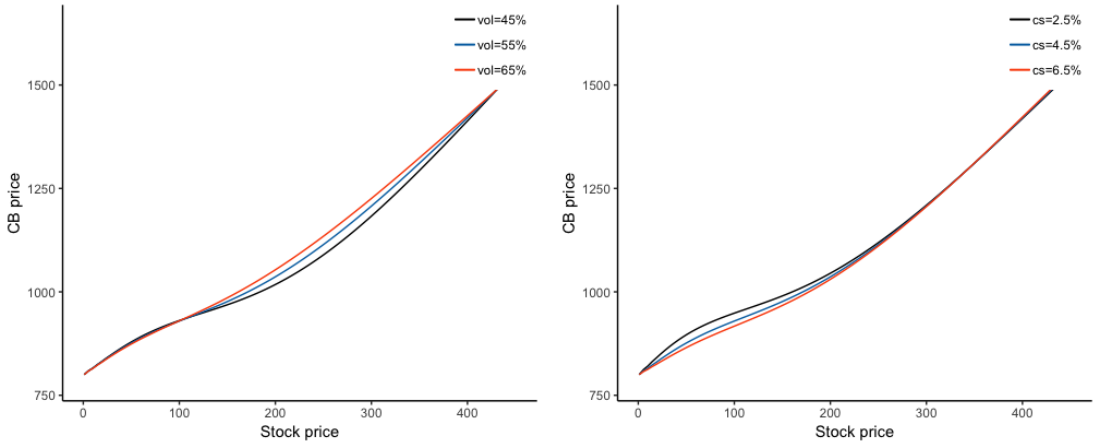

(c) Vol

(d) Cs

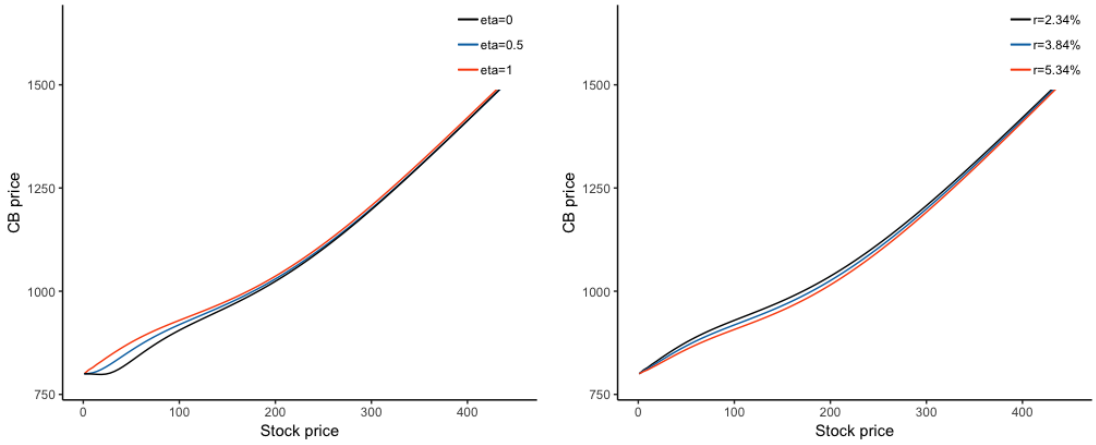

(e) η

(f) r

Figure E.1: Prce sensitivity to the different parameters; 1 yr to maturity, risk free rate=2.34%, volatility=55%, cs=0.045, R=0.8, dirty price per $1000

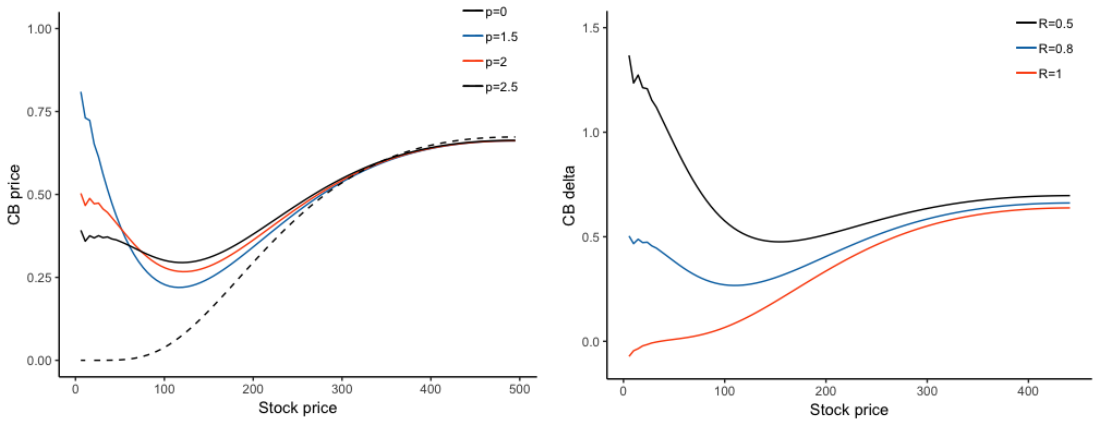

(a) p

(b) R

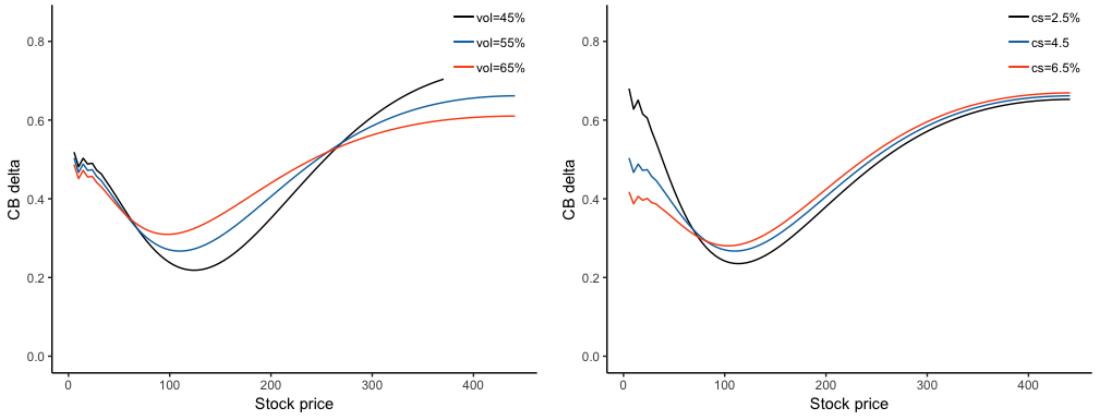

(c) Vol

(d) Cs

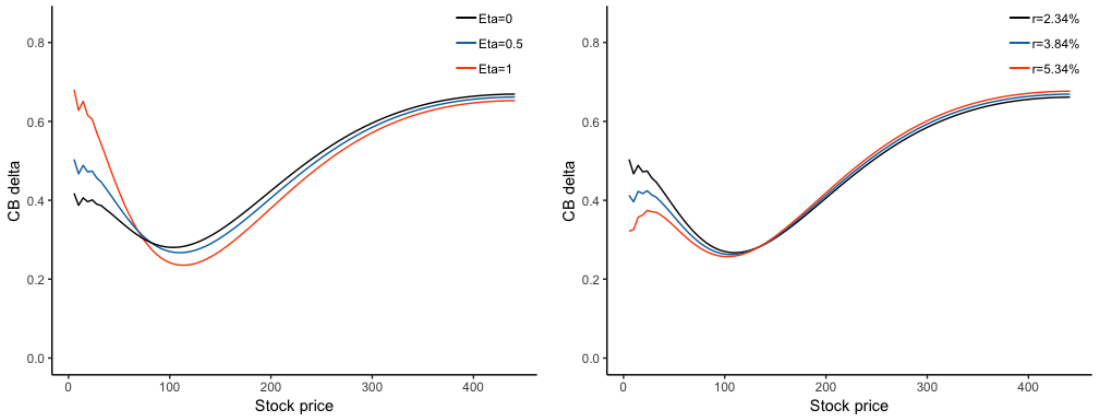

(e) η

(f) r

Figure E.2: Delta sensitivity to the different parameters; 1 yr to maturity, risk free rate=2.34%, volatility=55%, cs=0.045, R=0.8

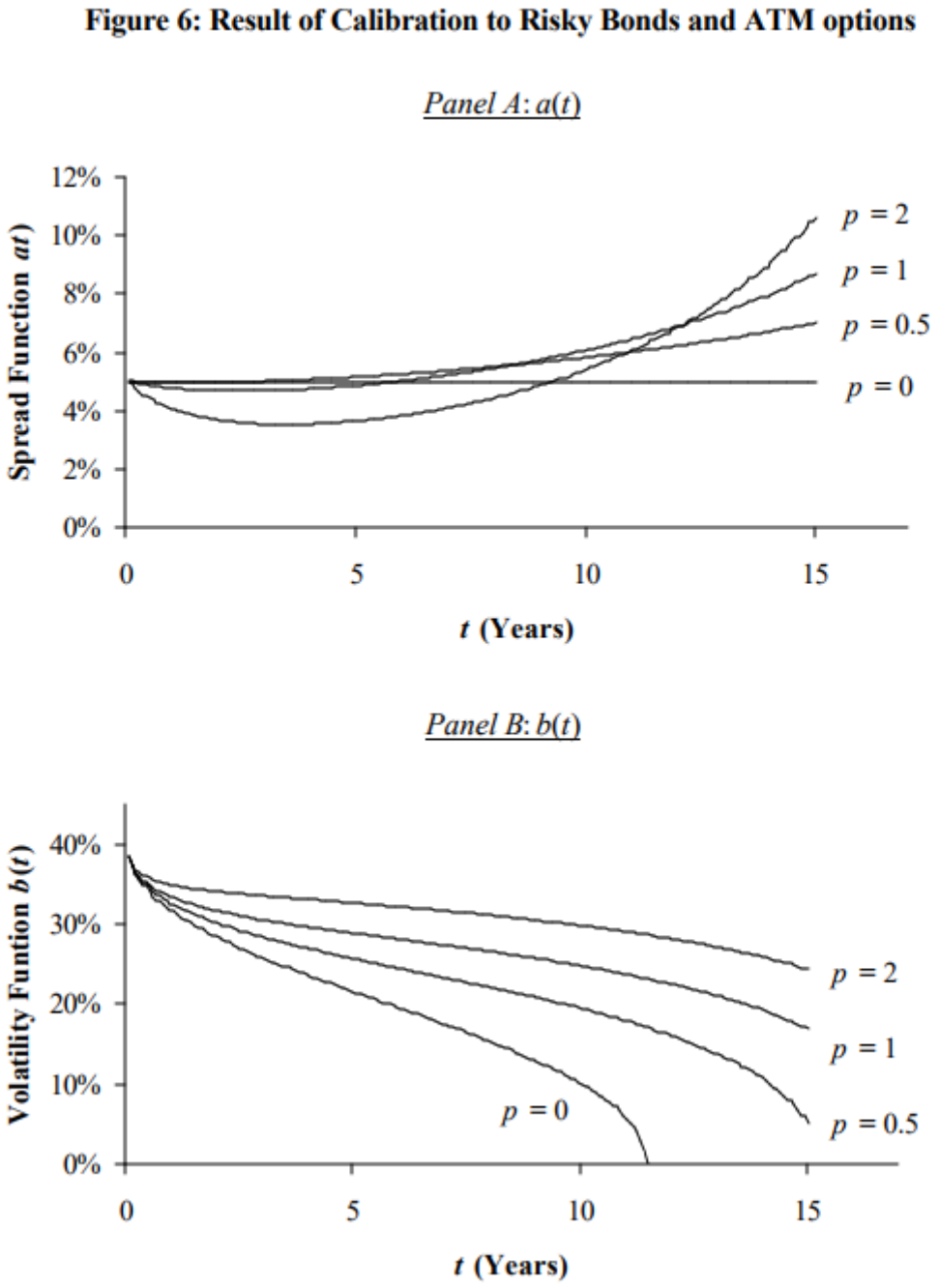

Figure E.3: Calibrated a(t) and b(t) for constant volatility and credit spread term structures equal to 40% and 5%, respectively (Andersen and Buffum, 2002, p. 36).

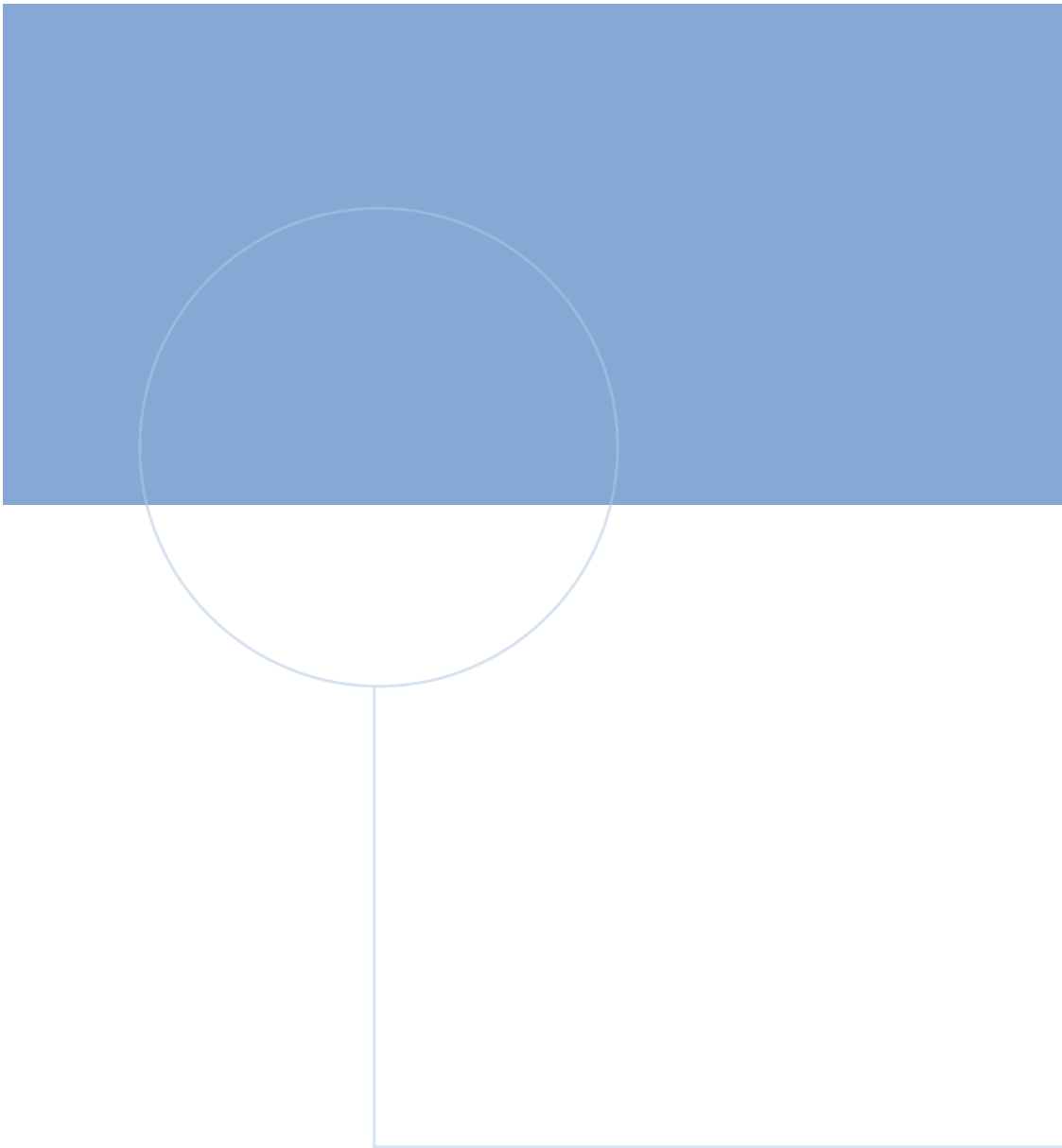

NTNU
Norwegian University of
Science and Technology